Water Air Soil Pollut (2026) 237:514
https://doi.org/10.1007/s11270-026-09207-8

Use of Free and Entrapped Spirogyra sp. Algae to Remove Endocrine-Disrupting Chemicals from Polluted Waters Through Biological Intervention

Gulay Bayramoglu · Ilkay Acikgoz-Erkaya · Omur Celikbicak · Mehmet Yakup Arica

Received: 16 June 2025 / Accepted: 24 January 2026
© The Author(s) 2026

Abstract Algae are used intensively in bioremediation studies due to their cell structure organization, doubling their weight in one day, ease of application in biotechnological processes, low cost, content of many useful substances, ability to remove some harmful substances from the environment, and resistance to environmental factors. In this work, *Spirogyra sp*. was isolated from freshwater sources in Ankara, and the cultivated algal biomass was entrapped in magnetic alginate beads (MA@ALG). The MA@ALG beads were used for the biosorption and degradation of three different endocrine-disrupting chemicals (EDCs), namely Bisphenol A (BPA), Diclofenac (DCF), and Congo red (CR), using free algal biomass as a control system. The biosorption capacities of the free algal biomass for BPA, CR and DCF were 89.4, 163.1, and 68.2 mg/g, respectively. Whereas the biosorption capacities of MA@ALG for BPA, DCF, and CR were 73.6, 104.4, and 49.5 mg/g, respectively. The presence of laccase-like activity of the *Spirogyra sp*. in the cell-free medium was assayed after contact with the EDCs. The degradation efficiencies of BPA, CR, and DCF were 79.7, 88.2, and 81.7% by the free algal biomass, and 68.9, 73.3, and 73.4% for MA@ALG, respectively, in a batch reactor for 7 days. Biosorption of BPA, DCF, and CR on the free algal biomass and MA@ALG is described by the Langmuir isotherm model and the pseudo-second order kinetic model. The toxicities of the tested compounds and degradation products were assessed with *Daphnia magna*, *Chlamydomonas reinhardtii*, and *Triticum aestivum L*. The degradation products of BPA, DCF, and CR had no remarkable toxic effect on the test organisms used compared to the parent compounds.

Keywords *Spirogyra sp.* · Entrapment · Magnetic alginate beads · Laccase · Biodegradation · Endocrine disturbing chemicals

G. Bayramoglu (✉) · M. Y. Arica (✉)
Biochemical Processing and Biomaterial Research Laboratory, Gazi University, 06500 Teknikokullar, Ankara, Turkey
e-mail: g_bayramoglu@hotmail.com

M. Y. Arica
e-mail: yakuparica@gmail.com

G. Bayramoglu
Department of Chemistry, Faculty of Sciences, Gazi University, 06500 Teknikokullar, Ankara, Turkey

I. Acikgoz-Erkaya
Department of Environmental Science, Faculty of Engineering and Architecture, Ahi Evran University, Kırsehir 40100, Turkey

O. Celikbicak
Department of Chemistry, Faculty of Sciences, Hacettepe University, 06800 Beytepe, Ankara, Turkey

1 Introduction

As is known, the primary source of energy used by all living things is solar energy, and the food chain begins

Published online: 06 February 2026

with the photosynthetic capabilities of eukaryotic and prokaryotic microalgae and other plant organisms. Algae can survive in many ecosystems ranging from sea to fresh water, from desert sands to hot springs, and together with fungi, they form lichens, the product of symbiotic relationships spread over very wide areas in different climatic conditions (Bayramoglu & Arica, 2023; Chaturvedi & Jaiswal, 2023a, 2023b; Otto et al., 2015; Selvan et al., 2023; Shing et al., 2018). Among algae species, *Spirogyra sp*. is a filamentous green microalga that lives in freshwater areas (Shing et al., 2018; Wijaya et al., 2025). These algae species are a renewable resource that can also eliminate toxic compounds from aqueous media and are used in the field of environmental biotechnology. The major organic pollutant substances in the aquatic environments are phenols, bisphenols, halogenated aromatics, polyaromatic hydrocarbons, pharmaceuticals, and dyes, toxic to humans and cause destruction of the liver, kidney, heart, and nervous system, and also, they are very toxic to aquatic living things (Bayramoglu et al., 2019, 2022; Liang et al., 2024; Rajaselvam et al., 2024; Tahraoui et al., 2024). Recently, their use in wastewater treatment has increased due to their easier harvesting route from freshwater compared to microalgae. Furthermore, *Spirogyra sp.* have also been used to remove metal ions from wastewater (Bayramoglu & Arica, 2011; Shing et al., 2018). Thus, these algal species can be used as efficient and favorable adsorbents due to their advantageous qualities. The major advantages are their extensive availability, low price, rapid adaptation to the biosorption process, and high reusability without leaving toxic substances behind (Al-Tohamy et al., 2022; Tahraoui et al., 2024). Moreover, some of them are EDCs that can mimic the biological activity of hormones. They can interact with the hormone receptors and affect the hormonal coordination. Among the EDCs, BPA, CR, and DF can be considered to be recalcitrant and persistent in the environment. BPA is extensively utilized for crosslinking polycarbonate, and slowly released from goods into the solutions. It has been classified as a harmful chemical due to its capability to destroy fertility and cause severe eye injury, allergic skin reactions, and respiratory irritation. Furthermore, BPA is an endocrine disruptor that can perturb the hormone system. CR is a benzidine-based dye that may play a role in disrupting various body functions. It is also noted to be involved in the induction of breast, testicular, and prostate cancers, as well as adverse effects on the endocrine system. The pharmaceutical "diclofenac" has also been reported to have endocrine-disrupting potential. Many studies have shown that diclofenac exhibits properties that produce physiological and behavioral effects on aquatic vertebrates, even at low concentrations. Several methods have reported for removal of these pollutants from aqueous solutions such as adsorption (Arica, et al., 2017a, 2017b; Chaturvedi & Jaiswal, 2023a, 2023b; Kumari et al., 2024; González-López et al., 2024; Saravanan et al., 2024; Bayramoglu et al., 2023; Tahraoui et al., 2024) reverse osmosis (Khazaali et al., 2014) photocatalytic degradation (Cai et al., 2024; Li et al., 2024; Moja et al., 2024) and adsorption-biodegradation (Bayramoglu et al., 2023; Modi et al., 2025). The latter method for removing toxic chemicals is resourceful, simple, and low-cost. Recently, numerous studies have been reported on adsorption-biodegradation, and further research is ongoing for novel biodegradation systems utilizing different microorganisms and enzymes. Among the microorganisms, algae are photosynthetic microorganisms that typically live in aquatic environments, soil, and other exposed places. Algae-based biodegradation can be a favorable process for the environmentally agreeable breakdown of many organic waste compounds. During the degradation process, algae can convert organic waste into water, carbon dioxide, and new biomass, which can be essential to the environment (Mustafa et al., 2021). Biodegradation is initiated through the interaction of algal enzymes with chemical compounds, resulting in the breakdown of chemical bonds within the pollutant compound structures. When it happens to biodegradation, the important parameters to contemplate are temperature, availability of light, oxygen, and moisture. Therefore, the use of inexpensive and easily produced algae for removing inorganic and organic pollutants from aqueous media constitutes an important alternative to traditional methods, due to several advantages, including the avoidance of environmental pollution and reduced energy consumption (Mustafa et al., 2021). Furthermore, when algal biomass is used in certain adsorption-biodegradation processes, some problems can arise that make it difficult to operate the process, such as difficulty in separating the biomass after adsorption and mass loss during regeneration. This difficulty can be addressed by entrapping the algal biomass in a loose hydrogel matrix

with minimal diffusion restrictions, such as alginate, a natural polysaccharide derived from brown algae. It was used in several studies for immobilization of different microorganisms (Touliabah et al., 2022; Xiong et al., 2018). The entrapped form of algal biomass can be more practical due to its easy separation from solutions and its reusability in batch and continuous reactor configurations.

Magnetic entrapment system can give notable advantages because it enables the easy separation of the composite adsorbent from the medium after the process. For example, poly(*o*-phenylenediamine) loaded magnetic carboxymethyl cellulose hybrid beads were synthesized and used for the removal of two model textile dyes (Arica et al., 2022). Agmatine and methionine functionalized magnetic alginate or magnetic alginate-activated carbon beads were utilized for the removal of various pollutants (Bayramoglu & Arica, 2024; Lilhare et al., 2021). Different alginate-based biosorbents were prepared and used for the removal of organic and inorganic pollutants (Bayramoglu & Arica, 2011).

In this study, environmentally friendly materials and methods were employed for the adsorption-biodegradation process of endocrine disruptors, including bisphenol A, Congo Red, and Diclofenac, which are among the most harmful pollutants to human health and the environment. In this study, Spirogyra sp. biomass was entrapped in magnetic alginate beads and utilized for the adsorption and biodegradation of three different EDCs. The presence of laccase-like activity of the *Spirogyra sp.* was determined in the cell-free medium after contact with the tested EDCs. ATR-FTIR, VSM, Zeta-sizer, light microscope, and UV–vis spectrophotometer were used for characterizing and analyzing the composite system and its biodegradation products. The effects of operational parameters on biodegradation, including pH, temperature, contact time, and the initial concentration of BPA, CR, and DCF, were also investigated. The toxicities of the degradation products formed during the biodegradation of three different endocrine-disrupting chemicals were also investigated.

2 Materials and Methods

2.1 Material

Bisphenol A, Congo red, Diclofenac sodium salt, sodium alginate (high-viscosity), and calcium chloride were obtained from Sigma-Aldrich Chemical Co. All the chemicals were of analytical grade and obtained from Merck AG (Darmstadt, Germany).

2.2 Growth Medium

A fresh algal culture of *Spirogyra sp.* was inoculated in 200 mL of Bold's basal medium (BBM) and incubated for 14 days at 25 °C in a rotary incubator at 100 rpm. It was illuminated 16/8 h of light/dark period using cool-white fluorescent (24W) and light intensity with a photon flux of 300 µmol photon m^{-2} s^{-1}. The BBM was inoculated with 0.2 g of algal cells to obtain a stock culture to be used throughout the research. The culture medium was oxygenated using an aquarium air pump. A light microscope photo of the algae was presented in Fig. 1.

2.3 Determination of the Growth Rate and Chlorophyll a + b Content of the Alga

The *Spirogyra sp*. growth was examined by weighing fresh alga mass as described previously. A specific method was applied to detect the fresh weights of the algal culture. Briefly, the culture was filtered under aseptic conditions, and weighed; the difference between the initial and final wet weight was determined. Chlorophyll a + b was determined as reported previously (Bayramoglu et al., 2019). Briefly, the

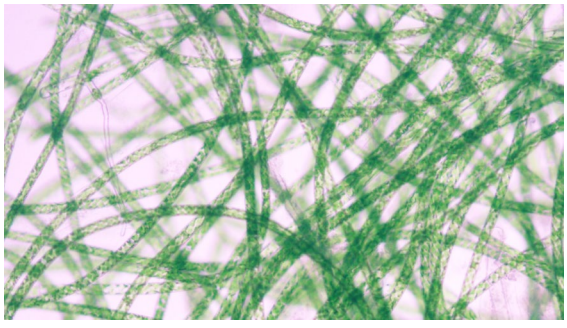


Fig. 1 Light microscope photo of *Spirogyra sp.* cells

Algae biomasses were collected by filtration. The algal biomass was re-suspended in methyl alcohol (4 mL) and sonicated for 5 min (Ultrasonic Cleaner, Model WF-UD2, 150 Watt, 50 Hz, Weigthlab Instruments, China), and incubated at 4 °C for 24 h under dark conditions, then the mixture was centrifuged again for 5 min at 14.000 rpm. The absorbance of the sample was measured spectrophotometrically at 652, 665, and 750 nm. Chlorophyll a + b concentration of each sample was calculated as described earlier (Porra et al., 1989).

2.4 Synthesis of Fe_3O_4 Magnetic Particles

The Fe_3O_4 particles were prepared as reported earlier (Arica & Bayramoglu, 2016). A $FeCl_3$ solution (150 mL, 0.3 mol/L) and an $FeSO_4$ solution (150 mL, 0.1 mol/L) were transferred to a flask and agitated at 25 °C for 1.0 h. After this period, the temperature was elevated to 70 °C, and NH_4OH (15,000 mL, 0.1 mol/L) was added to the medium, which was then refluxed for 3.0 h. Then, the temperature was raised to 90 °C further refluxed for 1.0 h. After the reaction was completed, the formed particles were separated using a magnet, cleaned with deionized water, and dried at 45 °C in a vacuum oven.

2.5 Immobilization of Algal Biomass in Magnetic Calcium-Alginate Beads

An alginate solution was prepared by dissolving 2.0 g of sodium alginate in 100 mL of BBM. Then, 1.0 g of magnetic particles and 0.5 g of chopped algal biomass were added and mixed with an overhead mixer for approximately 1.0 h. Then, the mixture was dropped into a $FeCl_3$ solution (0.1 mol/L) from a nozzle using a peristaltic pump, and the solution was stirred for an additional 30 min to stabilize the formed beads (~1.0 mm in size). When the sodium alginate, magnetic particle, and algal biomass combination was dropped into $FeCl_3$ solution, sodium ions were replaced with ferric cations to form an ionically crosslinked insoluble ferric cation-alginate gel. The formed magnetic composite beads (MA@ALG) were collected with a magnet and washed with 100 mL of BBM. Then, the composite beads containing algal biomass were incubated for 3 days to promote algal cell growth, as described above.

2.6 Biosorption Studies of Bisphenol A, Congo Red, and Diclofenac from Aqueous Medium

Biosorption can be described as a physicochemical procedure that takes place naturally on biomass preparations, which allows them to passively adsorb organic pollutants onto their cellular structure. Biosorption of BPA, CR, and DCF on the free algal biomass and MA@ALG was realized in a batch system. The biosorption rates and capacities of algal preparations were investigated. Stock solutions of the EDCs were prepared by dissolving BPA, CR, and DCF in deionized water (each 200 mg/L). For each biosorption study, 50 mg of free algal biomass or MA@ALG on a wet basis and 50 mL of EDCs were added to a vial and incubated in a rotary incubator at 25 °C and 150 rpm for 120 min. The initial and residual concentrations of the BPA, CR, and DCF in the sorption medium were determined spectrophotometrically at 270, 498, and 345 nm, respectively, in a UV–vis spectrophotometer (PG Instrument Ltd., Model T80 + ; PRC).

The sorption capacities of BPA, CR, and DCF on the free algal biomass and MA@ALG preparations were determined using the equation:

$$q = \left[\left(C_o - C_t\right)V\right]/M \quad (1)$$

where, q is the amount of the adsorbed BPA, CR or DCF by the free algal biomass and MA@ALG preparations (mg/g); C_o and C_t are the medium concentrations of the tested compound (mg/L) before and after biosorption, respectively, V is the volume of medium (L) and M is the weight of the biosorbent (g).

2.7 Determination of Laccase Activity after Contact with EDCs in the Algae Biomass

Laccase activity was determined using the Ride method, as described earlier (Bayramoglu et al., 2018), which involves the detection of a change in optical density during syringaldazine oxidation at 530 nm, utilizing a molar extinction coefficient of syringaldazine quinone of 65,000 M^{-1} cm^{-1}. Laccase activity determination was performed using a double-beam UV–vis spectrophotometer (Model T80 + ; PG Instruments Ltd., PRC).

2.8 Biodegradation of the BPA, CR, or DCF in a Batch System

Biodegradation is the process by which microorganisms, such as algae, bacteria, and fungi, break down organic compounds into their smaller units. Biodegradations of BPA, CR, or DCF were studied using free algae and MA@ALG preparations in a batch system with at different medium pH, and temperatures. For these experiments, BPA, CR, or DCF solution (50 mL) and either free algal biomass or MA@ALG (50 mg) were added to a vial and placed in a rotary incubator at 150 rpm and 25 °C for seven days. The medium pH was changed between 4.0 and 9.0. The initial concentration of EDCs in the solutions was 50 mg/L. The degradation efficiency of the algal preparations was assessed at four different temperatures (i.e., 15, 25, 35, and 45 °C), with an initial concentration of BPA, CR, or DCF of 50 mg/L. The initial and residual concentrations of the BPA, CR, or DCF in this medium were determined as described above.

2.9 MALDI-ToF- MS Studies

High-resolution mass spectra of BPA, CR, and DCF were obtained using a Matrix-Assisted Laser Desorption/Ionization Time-of-Flight Mass Spectrometry (MALDI-ToF–MS) system (Bruker, Billerica, MA, USA). The MALDI matrix, cyano-4-hydroxycinnamic acid solution (10 mg/mL), was prepared in a mixture of acetonitrile/water/trifluoroacetic acid (1:1:0.001, v/v/v). Sample solutions were mixed with matrices at a 1:10 v/v ratio by gentle stirring using a vortex. Then, 1.0 µL of the sample mixture was deposited onto the MALDI plates and dried; the plates were placed into the MALDI-ToF–MS system. MALDI analysis of the sample was performed in positive ion mode. The MALDI spectra were acquired by accumulating 5000 smart beam pulsed laser shots and were interpreted using Bruker FlexAnalysis software (Arica et al., 2017a, 2017b; Celikbicak et al., 2014).

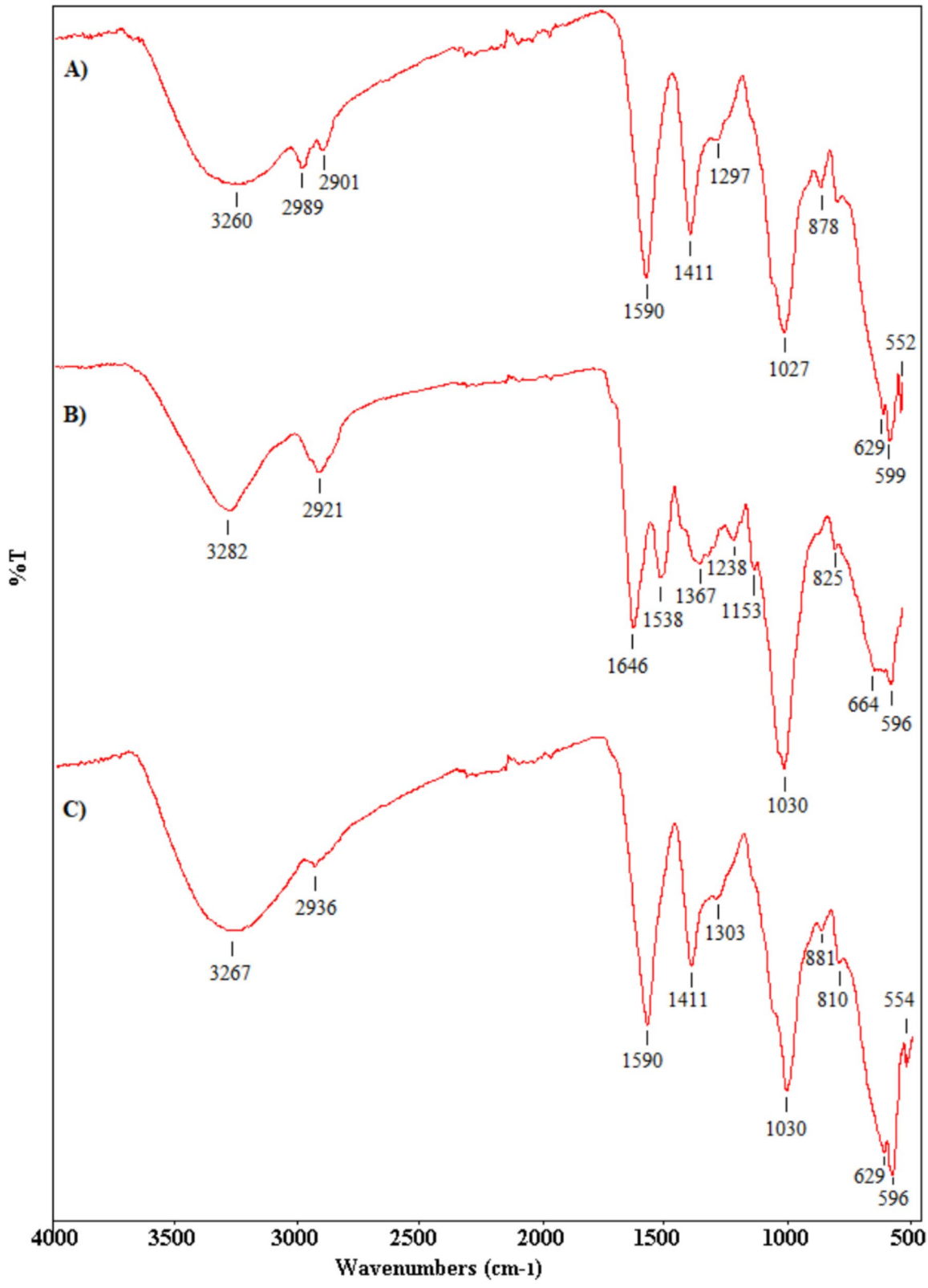
2.10 Characterization of Free Algal Biomass and MA@ALG Preparations

For the characterization of the free algal biomass and MA@ALG preparations, ATR-FTIR spectra were obtained using a Nicolet TM ISTM 50 spectrometer (Thermo Fisher Scientific, USA). The morphological appearance of the algal preparations was obtained using a light microscope. The magnetic properties of the magnetic particles and algal biomass-entrapped magnetic beads were obtained with a VSM (VSM, 880; ADE Technologies, USA). The zeta potential measurements of the free algal biomass, MA@ALG, and bare alginate beads at altered pH values were studied using a Zetasizer (Nano ZS, Malvern Instruments Ltd). The surface area and average pore size of the preparations were obtained via the Brunauer–Emmett–Teller (BET) analysis. The N_2 adsorption–desorption experiments were realized using ASAP2020 HD88. Analyses were performed by taking approximately 0.2 g from each sample. The moisture in the samples was removed using a degassing device at 50 °C for 12.0 h under reduced pressure. The measuring principle is based on the adsorption of nitrogen gas passed over the samples, and the calculation of the adsorbed amount of N_2 gas from the gas pressure.

The leakage of the ferric ions from the MA@ALG was also studied in the pH range of 5.0–8.0. The MA@ALG beads were incubated in solutions with different pH values while stirring at 25 ºC for 12 h, and the released Fe ions were determined in the supernatants using atomic adsorption spectrophotometry. The absorbance of the standard Fe ions and sample solutions was determined at a wavelength of 248.3 nm using a flame atomic adsorption spectrophotometry (AAS; Shimadzu AA 6800, Japan) with an air–acetylene flame. The slit width of the monochromator was 0.2 nm, and the absorbance reading was zeroed with pure water. Under these experimental conditions, any Fe ions released were not observed.

2.11 Toxicity of the Degradation Products of BPA, CR, or DCF

An acute immobilization study of *D. magna* was carried out according to the OECD report. Two different amounts of EDCs solutions were prepared, and daphnids were exposed to each EDC for 24 and 48 h, and the EC_{50} values were determined. Briefly, the toxicity studies were achieved by exposing the daphnids to two concentrations of BPA, CR, and DCF for 24 and 48 h. Ten daphnids were placed in 20 mL of each endocrine-disturbing solution with


A)
3260
2989
2901
1590
1411
1297
1027
878
629
599
552
B)
3282
2921
1646
1538
1367
1238
1153
1030
825
664
596
C)
3267
2936
1590
1411
1303
1030
881
810
629
596
554
%T
4000
3500
3000
2500
2000
1500
1000
500
Wavenumbers (cm-1)

◂**Fig. 2** FTIR spectra: Magnetic alginate beads **A**, *Spirogyra sp.* cells **B**, *Spirogyra sp.* cells entrapped in magnetic alginate beads **C**

two replicates. The surviving numbers of *D. magna* in each test were counted at 24 and 48 h time intervals (O.E.C.D, 2004). The survival rate was 100% in the control group. The EC_{50} values were designed as reported earlier (Alexander et al., 1988; Bayramoglu et al., 2019), and the EC_{50} value was calculated using the following formula:

$$EC_{50} = X_1 + \left[\left(50\% - Y_1\right)/\left(Y_2 - Y_1\right) \times \left(X_2 - X_1\right)\right] \quad (2)$$

Green algae growth inhibition test: Bold Basal Media (BBM) medium was used for the algae growth inhibition test according to the O.E.C.D., 2011 (O.E.C.D., 2011). Algae growth was realized at 25 ± 2 °C under 16:8 h of the light–dark cycle at 25 µmol m^2 s^{-1}. The algae cells were inoculated with two different BPA, CR, and DCF concentrations (i.e., 5 and 50 mg/L) in BBM medium, and the control groups did not contain EDCs. A standard phytotoxicity test was performed using Turkish winter wheat (*Triticum aestivum L.*) to assess seed germination and root elongation, as described earlier (25).

2.12 UV/Vis Spectrometry

The degradation of BPA, CR, and DCF was assessed by UV/vis spectrophotometer at 270, 498, and 345 nm for BPA, CR, and DCF, respectively. The percentages of endocrine-disrupting compounds degradation were calculated by absorbance obtained from the above-mentioned wavelengths before and after treatment of the chemicals with entrapped algal biomass. The formula used to calculate the percentage efficiency of EDCs is:

$$DegradationRate = \left[\left(C_o - C_t\right)/C_o\right] \times 100 \quad (3)$$

where C_0 is the initial concentration of the pollutant at time 0; C_t is the residual concentration of the pollutant at time t.

3 Results and Discussion

3.1 Characterization Studies

The use of cheap and easy-to-produce algae and entrapment in magnetic alginate for the removal of inorganic and organic pollutants from aqueous media constitutes an important alternative compared to traditional methods due to some advantages, such as not causing environmental pollution and being economically feasible. In this context, *Spirogyra sp.* biomass was entrapped in magnetic alginate beads as environmentally friendly materials and was used for the removal of endocrine disruptors such as bisphenol A, Congo red, and diclofenac via biosorption and biodegradation routes, which are the pollutants that are extremely harmful to human health and the environment.

The surface area and porosity of the free and MA@ALG beads were studied by nitrogen adsorption/desorption. The BET surface areas of the free and MA@ALG beads were found to be 11.3 m^2/g and 6.8 m^2/g, respectively. A large surface area was observed for the free algal biomass that provided high quantity of adsorption capacity for the pollutants. The average pore diameters for the free algal biomass and MA@ALG were found to be 54.2 nm and 71.6 nm, respectively. Thus, N_2 gas adsorption–desorption revealed the specific surface area and pore volume of the free algal biomass and MA@ALG beads. The surface area of the free algal biomass was 11.3 m^2/g, which was 1.7 times higher in comparison to MA@ALG.

The information about the chemical structure of the magnetic alginate (MA) and algal biomass entrapped beads (MA@ALG) was achieved using an FTIR spectrometer in the range of 400–4000 cm^{-1} (Fig. 2). The FTIR spectra of the MA are presented in Fig. 2A. The peak for the -OH group stretching vibration was detected at 3260 cm^{-1}, and the peak related to the $-CH_2$ group was observed at 2358 cm^{-1}. The peak at 1590 cm^{-1} was detected for the carboxyl group of alginate. The bands at 878 cm^{-1} and 1027 cm^{-1} could be related to the mannuronic acid and uronic acid functional groups of alginic acid. The peak at 639 cm^{-1} was attributed to the Fe_3O_4 particles in alginate beads. The broad band for the native *Spirogyra sp.* biomass at 3282 cm^{-1} could be recognized by the overlapping of the –OH and –NH

stretching vibration bands. The bands at 2921 cm^{-1}, 1646 cm^{-1}, 1538 cm^{-1}, 1367 cm^{-1}, 1030 cm^{-1}, and 596 cm^{-1} were seen in the spectrum of the native *Spirogyra sp.* biomass (Fig. 2B). The peaks at 1030 cm^{-1} and 1153 cm^{-1} exhibited characteristic correlations of C–O stretching vibrations in alcohol and amine groups on the algal biomass surface. Similar bands were observed in the spectra of MA@ALG beads as given in Fig. 2C.

The light microscope images were attained under a wet stage to evaluate the morphological properties of the bare alginate beads, MA and MA@ALG beads (Fig. 3, parts A, B, and C, respectively). All the preparations were more uniform and spherical in shape, approximately 1.0 mm in diameter. The MA@ALG beads displayed an irregular morphological structure compared to bare alginate and MA@ALG beads. Whereas algal biomass was observed uniformly distributed in the beads.

VSM data was used to display the magnetic properties of the Fe_3O_4, MA, and MA@ALG beads. S-shaped curves were obtained for Fe_3O_4, MA, and MA@ALG over the complicated magnetic field, demonstrating that the used samples had magnetic properties (Fig. 4). The magnetic performance of the Fe_3O_4, MA, and MA@ALG was found to be 42.4, 28.6, and 21.3 emu/g, respectively. The magnetic performance of the MA@ALG was slightly reduced due to the presence of algal biomass. The surface areas of the magnetic alginate beads, free algal biomass, and MA@ALG were determined with the N_2-adsorption–desorption isotherm, and their surface areas were found to be 12.7, 8.7, and 11.3 g/m^2, respectively. After entrapment of algal biomass in MA beads, the specific surface area of the MA@ALG was significantly increased. This could be due to the combination of the algal cells and the alginate polymer. The specific surface areas of all the samples were in the same order of magnitude.

The surfaces of algal cells have many different functional groups, such as $–NH_2$, =NH, -OH, -COOH, $-SO_3$, and $-PO_4$. The ionization states of these groups are altered on the algal cell surfaces according to the medium pH. In a study examining the biosorption of organic pollutants using biosorbent materials, it is crucial to determine both the pH value of the medium and the pH_{pzc} of the biosorbent used. Therefore, determining the pH_{pzc} value of the biosorbent is very important since the pH of

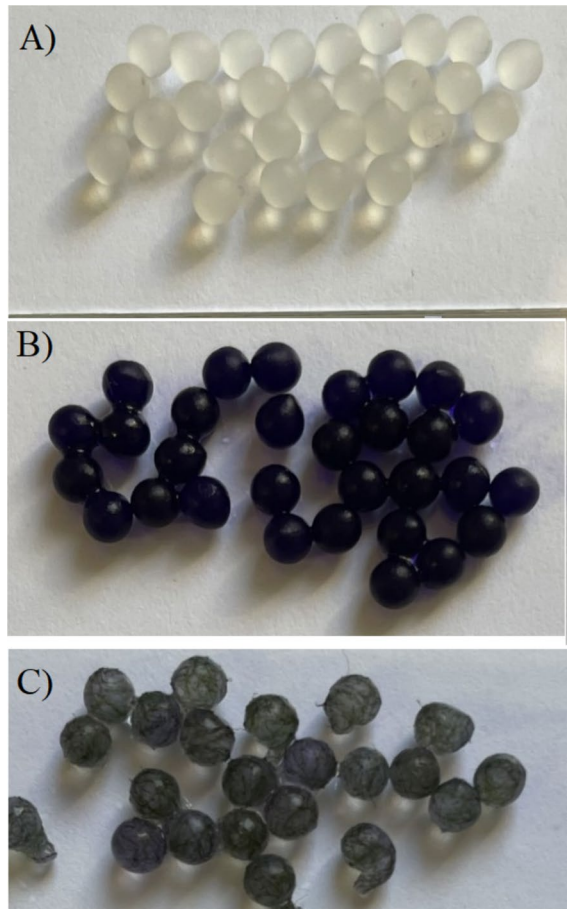


Fig. 3 Light microscope images: Bare alginate beads **A**, Magnetic alginate beads **B**; *Spirogyra sp.* cells entrapped magnetic alginate beads **C**

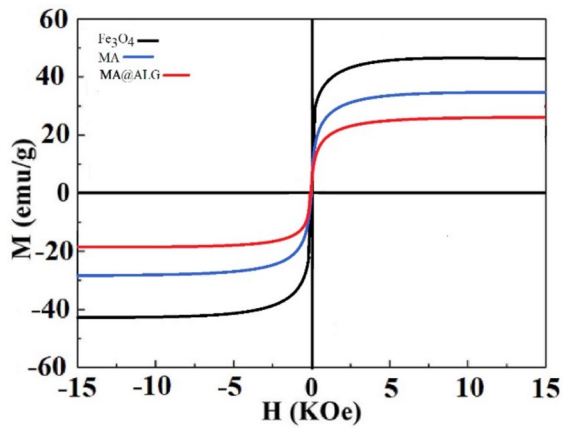


Fig. 4 The VSM analysis: Magnetic alginate beads **A**; *Spirogyra sp.* cells entrapped magnetic alginate beads **B**

the medium affects the surface charge properties of the biosorbent. The medium pH vs zeta potential values for the algal biomass and MA@ALG are shown in Fig. 5. Moreover, when the pH value of the medium exceeds the pHpzc of the biosorbent, its surface acquires a negative charge. Consequently, repelling or attracting organic pollutants, in general, with their cationic or anionic functional groups. The zeta potential values of the tested biosorbents steadily decreased with increasing pH, resulting in more net negative surface charge at elevated pH. The zeta potential plots for the magnetic alginate beads, free algal biomass, and MA@ALG displayed acidic surface properties as reported in earlier work (Bayramoglu et al., 2022). The zeta potential values of the magnetic alginate beads, free algal biomass, and MA@ALG decreased as the medium pH increased. As seen from the figure, the negative charge density of the MA@ALG was larger compared to the free algal biomass. The charge densities in the worked pH values were determined between 12.2 and −28.6 mV for the free algal biomass and 5.7 and −26.8 mV for MA@ALG. At pH between 2.0 and 4.0, the surface potentials of both samples were positive. The observed high negative zeta potential value for MA@ALG could be due to the carboxyl groups of alginate.

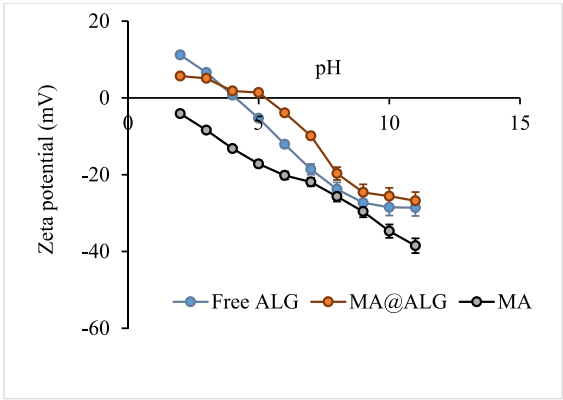


Fig. 5 Zeta potential of MA beads, free algae, and MA@ALG beads

3.2 Biosorption Studies of BPA, CR, and DCF from Aqueous Solutions

The surfaces of *Spirogyra sp.* cells contain many functional groups, allowing them to interact with pollutants in solution. The algal biomass can be used in both free and entrapped forms in loose hydrogels, and both forms can be involved in removing inorganic and organic pollutants from aqueous media (Bayramoglu et al., 2022; Gode et al., 2024; Rajaselvam et al., 2024). Here, the free and entrapped Spirogyra sp. biomass preparations were utilized for the biosorption of BPA, CR, and DCF from aqueous solutions. The effective parameters, such as biosorbent dose, pH, and the initial concentrations of the EDCs in the aqueous solution, were evaluated as the significant variables affecting the adsorption efficiency of the tested EDCs.

3.2.1 Effect of Biosorbent Dosage on BPA, CR, and DCF Biosorption

The effects of biosorbent dose in the range of 0.10–2.0 g/L on BPA, CR, and DCF biosorption by the free algal biomass and MA@ALG in an initial concentration of each compound of 100 mg/L, temperature of 25 °C, and at pH 6.0 were studied in a batch system. As seen in Fig. 6, increasing the biosorbent dosages for free algal biomass and MA@ALG beads from 0.1 to 2.0 g/L results in a substantial increase in the removal of all tested EDCs. Figure 6A and B show the effect of biosorbent dosage on the biosorption performance of the free algal biomass and MA@ALG that an increase in the percent removal of BPA, CR and DCF with the increase in the biosorbent amounts from and linearly increased from 0.1 to 1.0 g/L and the amounts of adsorbed BPA, CR and DCF were not significantly changed above the 1.0 g/L biosorbent dosage. In Fig. 6A, the amount of adsorbed BPA increased from 18.2 to 78.0%, CR from 25.5 to 96.4%, and DCF from 14.7 to 59.1% with an increase in the free algal biomass dosage from 0.1 to 1.0 g/L, respectively. Whereas the adsorbed amounts of BPA, CR, and DCF on the MA@ALG beads increased from 32.9 to 72.5%, from 40.6 to 78.4%, and from 21.8 to 47.1%, respectively (Fig. 6B). The enhancement in percent removal of BPA, CR, or DCF could be due to an increase in the number of accessible binding sites with the increasing

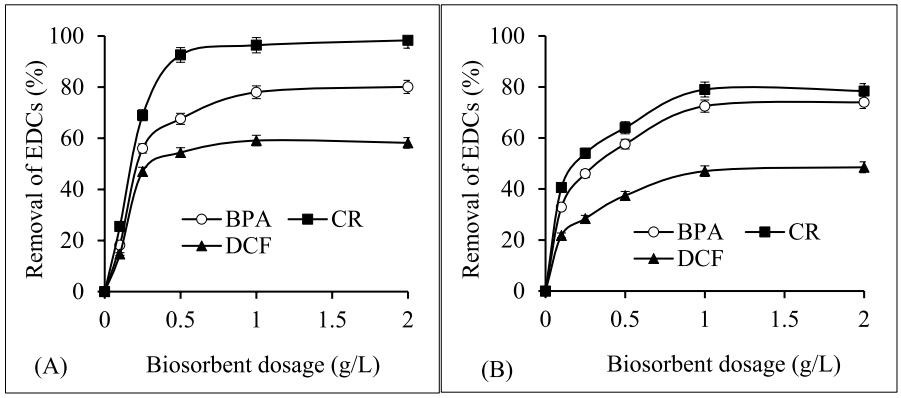


Fig. 6 Effect of biosorbent dosage on BPA, CR, and DCF sorption of the free algal biomass **A** and MA@ALG beads **B** (Initial concentration of ECDs compounds, 100 mg/L; temperature, 25 °C; contact time, 120 min; stirring rate 150 rpm)

biosorbent amount in the medium. On the other hand, the amount of adsorbed BPA, CR, or DCF per unit mass of the tested biosorbents decreased consistently with the increase in biomass amounts. This observation could be due to the binding sites of the tested biosorbent preparations not being completely employed by the tested EDCs. Hence, 1.0 g/L of free algal biomass or MA@ALG beads was utilized in the remaining endocrine-disrupting removal studies.

3.2.2 Effect of Medium pH on Biosorption Efficiency of BPA, CR, and DCF

The medium pH influences the ionization state of the functional groups on the biosorbent surface, such as -COOH, -PO4, -NH2, and=NH groups, as well as the solubility of the pollutant compounds. Generally, the surfaces of living algae cells are composed of negatively charged functional groups. The effect of pH on the biosorption efficiencies of BPA, CR, and DCF by the free algal biomass and MA@ALG beads was studied in the pH range 3.0–10.0. The results are shown in Fig. 7. As shown in the figure, the variation in medium pH resulted in an increase or decrease in the biosorption efficiencies of the free algal biomass and MA@ALG beads. The maximum biosorption capacity of the biosorbent was detected at 6.0 for all the tested EDCs. The amount of adsorbed BPA, CR, and DCF on the free algal biomass and MA@ALG beads progressively amplified with increasing medium pH from 3.0 to 6.0 (Fig. 7). As shown in the figure, the adsorption of BPA, CR, and DCF by the free algal biomass and MA@ALG beads was pH-dependent. The pK_a value of BPA is 9.78. Consequently, if the medium pH is less than the pKa values of the compounds, then these compounds are protonated. Here, BPA molecules are unprotonated state under the studied pH values. Therefore, the sorption of BPA on the tested biosorbents could result from the involvement of the hydrophobic, π–π electron donor–acceptor interrelationship and H-bond formations at the studied pH values. The

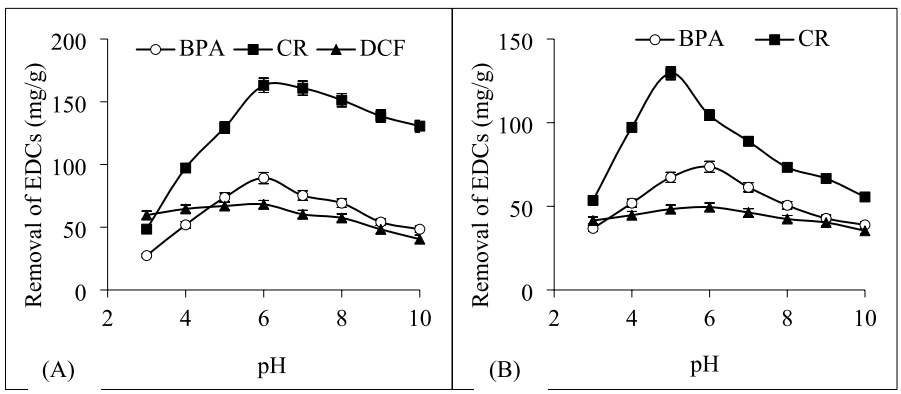


Fig. 7 Effect of pH on BPA, CR, and DCF biosorption of the free algal biomass **A** and MA@ALG beads **B** (Initial concentration of ECDs compounds, 200 mg/L; biosorbent dosage, 1.0 g/L; temperature, 25 °C; contact time, 120 min; stirring rate, 150 rpm)

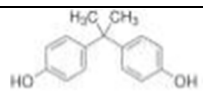
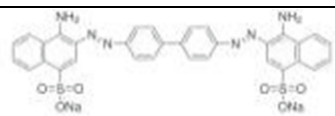
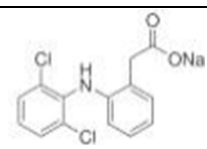
adsorption capacities of the free algal biomass and MA@ALG beads for BPA increased from 27.4 to 89.2 mg/g and from 36.8 to 73.6 mg/g, respectively, up to a pH of 6.0. Thereafter, the adsorbed amounts of BPA decreased as the medium pH increased from 6.0 to 10.0 for both the free algal biomass (from 89.2 to 48.4 mg/g) and the MA@ALG beads (from 73.6 to 38.9 mg/g), respectively. BPA molecules contain π-electrons that can interact with the unsaturated π-electrons on the aromatic benzene rings of the biosorbents, as well as the functional hydroxyl groups. Moreover, the π–π stacking interactions could be generated between the benzene ring of BPA and the aromatic moieties of the biosorbents.

CR is a benzidine-based dye and has two sulfates and two primary amino groups (Table 1). The pKa values of the sulfone and the amine groups of the dye are 1.87 and 8.52, respectively. Congo red dye is an amphoteric molecule, and at the studied pH values, both sulfone and amine groups are in the ionization state, and the hydronium ions compete with dye molecules to interact with the amine groups of the dye molecule. As shown in Fig. 7, the biosorption capacities of the algal biomass preparations for CR dye decreased at pH values above and below 6.0 for both the free algal biomass and MA@ALG beads. Maximum adsorption capacities of the free algal biomass and MA@ALG beads at pH 6.0 were found as.

163.1 and 104.4 mg/g, respectively. The amount of adsorbed CR dye increased with increasing medium pH from 3.0 to 6.0, and then progressively decreased above a pH value of 6.0, demonstrating that the amount of adsorbed CR dye was severely influenced by the medium pH.

The medium pH affected both the relative spread of the functional groups of the dye molecules and the adsorbent surface properties, and thus, the amount of adsorbed CR dye was determined. Furthermore, the

Table 1 Some properties of Bisphenol A, Congo red, and Diclofenac

	Bisphenol A	Congo Red	Diclofenac
H-bond donors	2	2	2
H-bond acceptors	2	12	3
EC number	201-245-8	209–358–4	239-346-4
Chemical formula	$C_{15}H_{16}O_2$	$C_{32}H_{22}N_6Na_2O_6S_2$	$C_{14}H_{10}Cl_2NNaO_2$
Molar mass (g/mol)	228.3	696.7	318.1
λ_{max} (nm)	270	498	345
Chemical structure			

amount of adsorbed CR dye on the biosorbent preparations could be affected by the electrostatic interactions between the deprotonated sulfone groups and the zwitterion form of dye and the tested biosorbents. DCF sorption by the free algal biomass and MA@ALG beads was also studied as a function of medium pH. DCF is a weak acid with a pK_a value of 4.0 and has a limited solubility in water.

As given in Fig. 7, the adsorption capacities of the free algal biomass and MA@ALG beads for DCF were not changed significantly at pH between 3.0 and 4.0; the amount of DCF biosorption was found to be 68.2 and 48.6 mg/g at pH 6.0, respectively. At pH < 4.0, the carboxyl groups of DCF molecules are not deprotonated, and their solubility is decreased in the medium. Whereas above pH 4.0, the DCF molecule has a negative charge. The pH_{pzc} values of native and entrapped algal biomasses were 8.7 and 9.4, respectively. Thus, the biosorbent and the acidic characteristics of DCF indicate that DCF biosorption could be assured for pH below the biosorbent's pH_{pzc}. In this work, the biosorption efficacy was maximum at pH 6.0 for both tested biosorbents. As is well known, medium pH is a critical parameter that not only affects the surface charge distribution of the adsorbate but also changes the surface charge of the biosorbent due to functional group dissociation. The surface charge of the algal cells has been reported to be negative. The reduction in the biosorption amount of DCF can be attributed to its presence in the protonated form at low pH values ($pK_a = 4.0$). Conversely, at pH values higher than its pK_a value, it has a negative charge. In addition, DCF could interact with the algal cells' surface and act as a good host for DCF through noncovalent interactions with its carboxyl groups, resulting in higher adsorption.

3.3 Influence of the Initial Concentration of BPA, CR, and DCF on the Biosorption Capacities and Isotherm Studies

Figure 8 shows the effect of the initial BPA, CR, and DCF concentrations on the biosorption performance of the free algal biomass and MA@ALG beads from aqueous solutions. As observed from this figure, an increase in the initial concentration of BPA, CR, and/or DCF from 5.0 to 200 mg/L leads to significant changes in the biosorption performance of the biosorbents. Generally, a high concentration of adsorbate in solution intensifies the contact of the solute molecules with the binding sites of the biosorbent. Thus, this event can supply a greater removal performance with a high adsorption capacity. Thus, the adsorption capacities of the free algal biomass and MA@ALG beads gradually amplified until the initial concentration of the tested pollutants reached 200 mg/L. This could result from the presence of appropriate binding sites for the adsorbate molecules on the biosorbent surfaces at a lower concentration of the solute. For free algal biomass, the biosorption capacity increased from 3.5 to 89.4 mg/g for BPA, from 4.9 to 163.1 mg/g for CR, and from 3.9 to 68.2 mg/g for DCF, respectively. Whereas the biosorption capacities of entrapped algal biomass were amplified for BPA from 4.8 to 73.6 mg/g, for CR from 4.2 to 104.4 mg/g, and for DCF from 2.7 to 49.5 mg/g. The MA@ALG beads significantly improved the removal performance of the tested pollutant compounds. The high

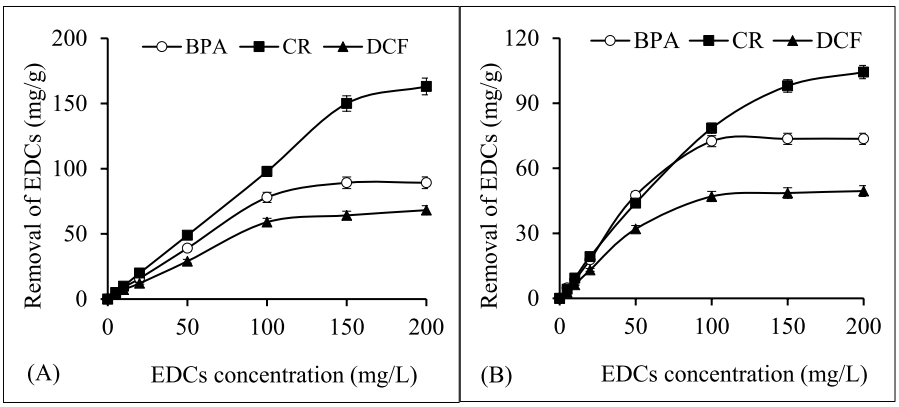


Fig. 8 Effect of initial concentrations of BPA, CR, and DCF on biosorption of the free algal biomass **A** and MA@ALG beads **B** (Biosorbent dosage, 1.0 g/L; temperature, 25 °C; contact time, 120 min; stirring rate, 150 rpm)

biosorption capacity of the free algal biomass for BPA, CR, and DCF was attributed to its high surface area, which is greater than that of MA@ALG beads. The BET surface area of the free algal biomass was 1.7 times greater than that of the MA@ALG beads. The experimental biosorption capacities of the free algal biomass were observed to be greater than 1.21%, 1.56% and 1.37% for BPA, CR, and DCF, respectively, compared to MA@ALG beads. From these results, the surface area of biosorbents was observed to be an important factor for affecting the biosorption capacity.

The biosorption of BPA, CR, and DCF on the free algal biomass and MA@ALG beads was characterized by applying two isotherm models to designate the experimental data. Equilibrium data, usually known as biosorption isotherms.

The equation for the Langmuir and the Freundlich biosorption isotherm model:

$$q_e = q_m C_e / \left(K_d + C_e\right) \tag{4}$$

$$q_e = K_F \left(C_e\right)^{1/n} \tag{5}$$

The Langmiur plots were obtained for the free algal biomass and MA@ALG beads and the R^2 values were in the range of 0.957–0.997 and 0.979–0.998, respectively (Table 2). From the table, the theoretical values of q_m for the free algal biomass and MA@ALG beads were very close to the experimentally achieved biosorption capacities (q_{exp}). Therefore, the biosorption of BPA, CR and DCF molecules on both biosorbents can be well elucidated by the Langmuir model. Experimental data attained for the biosorption of BPA, CR, and DCF molecules on the free algal biomass and MA@ALG beads were designed according to the Freundlich isotherm model, and the Freundlich isotherm parameters, such as n and K_F, and the correlation coefficients (R^2) were calculated (Table 2). The obtained theoretical values did not fit the Freundlich isotherm for both tested biosorbents. Here, the obtained K_F values do not reflect the total biosorption capacity, but are reflected as a comparative amount of biosorption under certain conditions.

3.4 Biosorption Time of BPA, CR, and DCF on Biosorbents and Kinetic Studies

The adsorption equilibrium time of BPA, CR, and DCF on the free algal biomass and MA@ALG beads was obtained approximately at 120 min with an initial concentration of each compound of 200 mg/L (Fig. 9). As shown in this figure, the data displayed that a two-stage biosorption kinetic route took place for the free algal biomass and MA@ALG beads. In the early stage, a very fast adsorption rate was detected within 20 min, then, followed by a moderate adsorption period till 120 min. In the early stage, for the free algal biomass and MA@ALG beads, approximately 79.0 and 62.7% of BPA, 153.3 and 98.1% CR, and 61.3 and 48.4% DCF were adsorbed within 20 min, respectively. At the initial stage of the biosorption process, the available binding sites for the pollutant compounds are progressively employed, after which the pollutant biosorption rate is reduced and reaches biosorption equilibrium. Similar findings in the biosorption rate have also been reported previously for different biomasses in the removal of

Table 2 Langmuir and the Freundlich isotherm model constants and correlation coefficients were determined in the biosorption process of EDCs to the free algal biomass and MA@ALG beads

Biosorbent		Langmuir constant						Freundlich constant				
	EDCs	$q_{e,exp}$ (mg/g)	q_m (mg/g)	$K_d x10^{-2}$ (mg/L)	R^2	χ^2	RMSE	n	K_F	R^2	χ^2	RMSE
Free algal biomass	BPA	89.4	112.7	0.229	0.957	4.73	12.6	1.49	5.91	0.930	28.5	38.7
	CR	163.1	170.7	0.017	0.997	0.298	4.03	2.67	48.1	0.616	61.9	78.6
	DCF	68.2	87.2	0.317	0.982	4.21	9.79	1.58	3.94	0.985	6.74	11.5
MA@ALG beads	BPA	73.6	77.3	0.050	0.998	0.184	2.17	2.30	12.6	0.903	13.1	21.9
	CR	104.4	116.8	0.108	0.990	1.26	6.85	2.44	11.5	0.920	9.92	7.03
	DCF	49.5	61.6	0.295	0.979	2.38	6.08	1.51	2.67	0.939	10.4	14.1

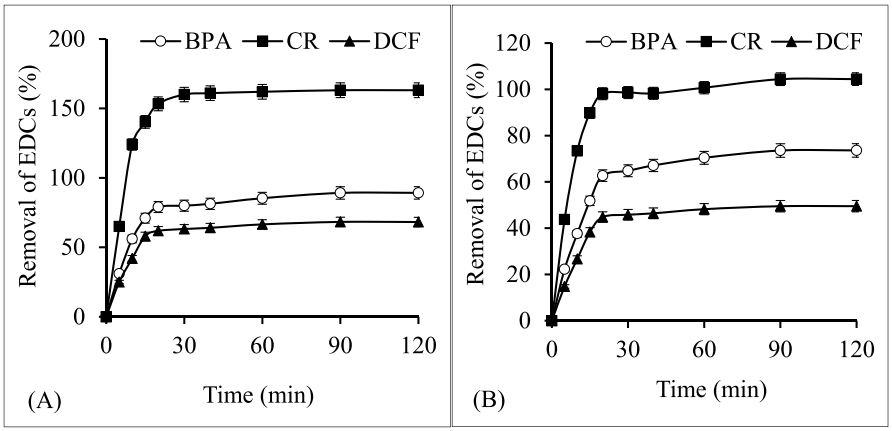


Fig. 9 Effect of time on BPA, CR, and DCF biosorption of the free algal biomass **A** and MA@ALG beads **B** (Initial concentration of ECDs compounds, 100 mg/L; biosorbent dosage, 1.0 g/L; temperature, 25 °C; stirring rate 150 rpm)

multipart phenolic compounds (Bayramoglu et al., 2023; Semwal et al., 2024; Wlizło et al., 2024). In the literature, a varied range of biosorption times has been stated for the removal of BPA, CR, and DCF with diverse biosorbents (Bayramoglu & Arica, 2023). In the presented study, a rapid biosorption rate was observed for both biosorbents, with an equilibrium biosorption time of approximately 120 min.

The pseudo-first- and second-order kinetic models were established to evaluate the biosorption process of the free algal biomass and MA@ALG beads.

The first-order kinetic model equation:

$$d_{qt}/d_t = k_1\left(q_e - q_t\right) \tag{6}$$

$$\log\left(q_e - q_t\right) = \log q_e - \left(k_1.t\right)/2.303 \tag{7}$$

The linear form of the second-order equation:

$$t/q_t = 1/\left(k_2 {q_e}^2\right)t + 1/q_e \tag{8}$$

The calculated parameters of the pseudo-first- and second-order kinetic models are presented in Table 3. The calculated R^2 values of the second-order equation were in the range of 0.997–0.998 for the tested biosorbents, while the R^2 values of the first-order kinetic model were found to be in the range of 0.903–0.956. Moreover, the calculated biosorption capacity (q_e) realized from the second-order kinetic equation for BPA, CR, and DCF on the free algal biomass and MA@ALG beads was very close to the experimental findings (q_{exp}). Thus, the biosorption of BPA, CR, and DCF on the free algal biomass and MA@ALG beads was better described by the second-order kinetic model compared to the first-order kinetic model. These results are in agreement with earlier studies of BPA, CR, and DCF biosorption using various microbial biomasses (Bayramoglu et al., 2022; Daniel et al., 2025).

Table 3 First and second order kinetic parameters for the adsorption of EDCs to the free algal biomass, and MA@ALG beads

Biosorbent		First-order						Second-order				
	EDCs	$q_{e,\,exp}$ (mg/g)	q_{eq} (mg/g)	$k_1\times10^2$ (min^{-1})	RMSE	χ^2	R^2	q_{eq} (mg/g)	$k_2\times10^3$ (g/mg/min)	RMSE	χ^2	R^2
Free algal biomass	BPA	89.4	127.9	7.411	22.6	11.9	0.903	94.8	1.63	3.51	0.33	0.998
	CR	163.1	50.1	6.75	64.2	253	0.956	169.9	1.46	3.62	0.21	0.999
	DCF	68.2	109.8	13.3	23.9	15.1	0.907	72.1	3.49	2.14	0.19	0.999
MA@ALG beads	BPA	73.6	128.2	9.69	31.5	23.7	0.929	80.3	1.38	3.75	0.58	0.999
	CR	104.4	70.6	8.39	19.8	16.8	0.912	108.8	2.14	2.38	0.20	0.998
	DCF	49.5	120.4	12. 5	41.7	41.3	0.918	53.6	2.50	2.06	0.29	0.997

Two statistical error functions were selected to validate the best biosorption models for both isotherm studies and kinetic (Ghibate et al., 2025). Both the free algal biomass and MA@ALG beads' predictive efficiencies regarding EDCs biosorption were statistically assessed by calculating the chi-square test statistic ($\chi 2$) and RMSE to establish a ranking of their performance.

The chi-square test statistic (χ^2) is essentially the sum of the squares of the differences between the experimental data referred to as the observed values ($q_{exp,i}$) obtained by calculating from models called the predicted values ($q_{m,i}$), with each squared difference divided by the corresponding data obtained from models (Eq. 9).

$$\chi_2 = \sum_{(i=1\to N)} \left[\left(q_{exp,i} - q_{m,i}\right)^2 / q_m \right] \quad (9)$$

where N is the number of experimental data points.

The root-mean-square error (RMSE), as a corresponding error function equation, is presented in Eq. (10).

$$RMSE = \left[(1/N) \sum_{i=1\to N} \left(q_{exp,i} - q_{m,i}\right)^2 \right]^{1/2} \quad (10)$$

The determination coefficient (R^2), root mean square error (RMSE), and the Chi-square test statistic (χ^2) for both isotherm and kinetics models used to describe the EDCs biosorption at a temperature of 298 K are presented in Tables 2 and 3. As shown in Table 2, the Langmuir model, compared to the Freundlich model, is considered the best model for describing EDCs biosorption, as it yields the highest R^2 value, the lowest RMSE, and a significant chi-square test result. A similar evaluation also remained valid for the evaluation of first- and second-order kinetic equations (Table 3). To evaluate the fitting of the isotherm models with experimental equilibrium data in isotherm and kinetic studies, error functions were used. The outcomes of different error functions, including χ^2 and RMSE, were computed to determine the most suitable error function for the system. The data presented in Table 2 provide key insights into the performance of the Langmuir and Freundlich adsorption isotherms. The high correlation coefficient for the Langmuir model ($R^2 = 0.957–0.982$ for the free algal biomass, and $R^2 = 0.979–0.998$ for the MA@ALG beads), which is significantly higher than that of the Freundlich model ($R^2 = 0.616–0.985$ for the free algal biomass, and $R^2 = 0.903–0.939$ for the MA@ALG beads), suggests that the Langmuir isotherm offers an excellent fit to the experimental data. Additionally, as shown in Table 2, the calculation of the error value indicates that the Langmuir model provides a better fit to the experimental data. The Langmuir model shows lower error values (RMSE = 4.03–12.6 for the free algal biomass, and RMSE = 2.17–6.85 for the MA@ALG beads; $\chi^2 = 0.298–4.73$ for the free algal biomass, and $\chi^2 = 0.184–2.38$ for the MA@ALG beads) compared to the Freundlich model (RMSE = 11.5–78.6 for the free algal biomass, and RMSE = 7.03–21.9 for the MA@ALG beads; $\chi^2 = 6.74–28.5$ for the free algal biomass, and $\chi^2 = 9.92–13.1$ for the MA@ALG beads). The agreement between the equilibrium experimental data and the linear Langmuir model equation analyses during the biosorption process supports the conclusion that the Langmuir model better represents the adsorption of EDCs onto free algal biomass and MA@ALG beads. The fit between the experimental and theoretical data was assessed by comparing the regression coefficients (R^2) and the calculated adsorption capacities with the experimental values. Furthermore, statistical error analysis was performed, incorporating error functions such as the root-mean-square error (RMSE) and the chi-square test (χ^2) to evaluate the equilibrium models with maximum precision. The findings in Table 3 indicate that the biosorption of EDCs onto the free algal biomass and MA@ALG beads follows the second-order kinetics, as the R^2, χ^2, and RMSE values obtained are better than those for the first-order kinetics, thus suggesting the heterogeneity of the biosorbents' sorption sites. These findings, supported by the equilibrium experimental data in Figs. 8 (partly A and B) and 9 (partly A and B), confirm that the Langmuir and second-order kinetic models, respectively, more accurately describe the biosorption behavior observed in this study.

3.5 Biosorption Mechanisms of BPA, CR, and DCF on Biosorbents

Algal biomasses essentially consist of polysaccharides (namely, polycolloids, alginates, and carrageenans) and proteins, which play a major role in binding

pollutants to the cell surface (Shtein et al., 2018). Accordingly, the proposed biosorption mechanism for BPA, CR, and DCF on the algal biomass preparations (*Spirogyra sp.*) involves the interaction between the amine, hydroxyl, carbonyl, carboxyl, phosphate, and sulfate groups of green algae and the functional groups of tested EDCs (Bayramoglu & Arica, 2023; Wlizło et al., 2024). Hence, the biosorption of BPA, CR, and DCF can occur through H-bonding, electrostatic interactions, ion-exchange, and π-π interactions. As shown in the FTIR spectra, the hydroxyl and amine functional groups were detected for algal biomasses at 3267 cm^{-1}, and they could be responsible for the hydrogen bonding interactions and affect the biosorption capacities of the free algal biomass and MA@ALG beads to BPA, CR, and DCF. Moreover, the bands at 1646 and 1538 cm^{-1} could be attributed to π–π interactions. The BPA molecule has two H-bond donors and two pendant hydroxyl groups, the CR molecule has two H-bonds, twelve H-bond acceptors, two primary amine groups and two sulfone groups, and the DCF molecule has two hydrogen bond donors, three hydrogen bond acceptors, a secondary amine and a carboxyl group. They also have several hydrophobic entities. Conversely, the free algal biomass and MA@ALG beads have many acidic, basic functional groups and hydrophobic entities. Hence, BPA CR and DCF molecules can be adsorbed onto algal biomass preparations through H-bonding, ion-exchange, and π–π interactions. The aromatic rings of BPA, CR, and DCF may form π–π interactions with the π bonds on the biosorbents, thereby enhancing the biosorption capacities of the biosorbents. Moreover, the aromatic structures of the tested EDCs not only exhibited a strong π–π interaction but also showed a high van der Waals interaction with the biosorbents, thereby increasing the adsorption capacity of the adsorbents (Bayramoglu et al., 2022; Liang et al., 2024). The aromatic rings of BPA, CR, and DCF generate π–π interactions with the π bonds on the algal cell wall compounds, which can enhance the biosorption capacities of the algal biomass preparations. Moreover, the aromatic structures of the tested EDCs can not only interact with a strong π–π interaction but also form a high van der Waals interaction with the tested biosorbents, thereby enhancing the biosorption performance of the biosorbents (Bayramoglu et al., 2022; Liang et al., 2024). Furthermore, CR and DCF have two negatively charged sulfone groups, two positively charged amine groups, and a negatively charged carboxyl group, respectively. Consequently, these functional groups on CR and DCF interact with algal biomass preparations via ion-exchange interactions, which play a crucial role in increasing the biosorption capacity of algal biomass preparations. Thus, the respective functional groups of BPA, CR, and/or DCF molecules (i.e., hydroxyl, amine, carboxyl, sulfone, and hydrophobic groups) interact with algal biomass preparations, resulting in high biosorption capacity for these preparations. Consequently, the presence of hydrogen acceptors (–C = O at 1030 cm^{-1}) and hydrogen donor groups (–NH_2 at 1646 cm^{-1}) on the surface of the fungal biomass preparations can form hydrogen bonds with targeted EDCs, thus reinforcing the biosorption interactions. Furthermore, the high number of functional groups on the tested biosorbents provides more active sites for interaction with the target EDCs, resulting in a substantial enhancement in biosorption performance.

3.6 Reusability of the Free Algal Biomass and MA@ALG Beads for Biosorption of ECDs

The reusability of the free algal biomass and MA@ALG beads is a crucial parameter that needs to be investigated for the cost-effectiveness of BPA, CR, and/or DCF biosorption from aqueous media. For this reason, five consecutive biosorption/desorption cycles of the free algal biomass and MA@ALG beads were performed to remove the tested EDCs from the aqueous media. Ethanol (10%) and a low-concentration HNO_3 solution (20 mmol/L) were used for desorption of BPA, CR, or DCF from the surface of the biosorbents (data not shown). After five cycles, the biosorption capacities were found to be 71.5% and 77.8% for BPA, 76.7% and 86.4% for CR, and 77.3% and 84.2% for DCF with the free algal biomass and MA@ALG beads, respectively. These results were rational and appropriate; the reusability performance shows that the algal biomass preparations can be recycled for the treatment of polluted water.

3.7 Laccase Enzyme Activity

The laccase-like activity of the cell-free extract from Spirogyra sp. was determined using syringaldazine as a substrate, as previously reported (Bayramoglu et al.,

2019). A notable laccase-like activity was detected in BPA, CR, and DCF-treated free algal biomass compared to the control algal biomass cell-free extract. The medium containing Congo red dye, a maximum laccase activity, was determined compared to BPA and DCF. The maximum laccase activity was 403 U/mL with Congo red, followed by 324 U/mL and 205 U/mL with BPA and DCF, respectively. The order of the detected laccase activity was CR > BPA > DCF. Any laccase-like activity was not determined in the cell-free extract of the algae growing in pure medium. These results showed that the detected laccase-like enzyme played an important role in the degradation of the three EDCs. Laccase-like activity has also been reported in the cell-free extracts of other algal species during the biodegradation of aromatic pollutants in the literature (Otto et al., 2015; Selvan et al., 2023).

3.8 Effect of BPA, CR, and DCF on the Chlorophyll a + b Content of *Spirogyra sp*

Chlorophylls play a major role in the photosynthesis process, and the chlorophyll molecule contains a porphyrin ring, a magnesium atom at the center, and a hydrocarbon phytol chain. Three types of pigments are present in the algae, namely, chlorophylls, carotenoids, and phycobilin proteins. Chlorophyll a is the light-harvesting pigment, whereas Chlorophyll b helps Chlorophyll a. The amounts of chlorophyll a + b were determined in algae cultures after incubation for seven days with two different concentrations of BPA, CR, and DCF, using pristine algal culture as a control. Control algal culture displayed an increase in chlorophyll a + b content during the exponential growth phase, up to seven days, and gradually decreased until fourteen days. The decrease in the chlorophyll a + b content of the algal culture could be due to nutrient deficiency. As given in Table 4, there was no significant change in the amount of chlorophyll a + b content in the culture containing 5.0 mg/L of BPA, CR, and DCP compared to control groups, and these results showed that the existence of these endocrine disturbing at low concentration did not produce any negative effect on chlorophyll a production during the growth phase of *Spirogyra sp*. Similar observations have been stated in the literature. For example, Wilt et al. studied the effect of diclofenac on the chlorophyll a content of *Chlorella sorokiniana* and reported that the presence of a pollutant mixture at concentrations between ~ 100 and 350 µg/L did not alter the chlorophyll a content (de Wilt et al., 2016). On the other hand, the algal culture showed a decrease in the chlorophyll a + b content at 50 mg/L of BPA, CR, and DCF concentration compared to the control algal culture (Table 4). The total amounts of chlorophyll a + b content were found to be 33.9%, 39.4%, and 47.2% for BPA, CR, and DCP, respectively, at their initial concentrations of 50 mg/L. Thus, *Spirogyra sp.* were exposed to different EDCs for seven days, and a strong reduction in the total chlorophyll a + b content was observed (Table 4), demonstrating a decrease in total chlorophyll synthesis. A lower amount of chlorophyll a + b was observed in *Spirogyra sp*. for BPA at 50 mg/L, when compared to the other two endocrine-disrupting compounds. As observed in this table, chlorophyll a + b content is dependent on the mass of the algal cell in the medium and the concentration of EDCs. The amounts of harvested biomass of *Spirogyra sp.* at two different BPA, CR, and DCP concentrations are presented in Table 4. The lower amount of biomass was harvested with BPA in 50 mg/L by *Spirogyra sp.* (0.316 ± 0.044 mg/L), compared to the two other EDCs.

Table 4 Biomass and total chlorophyll (a + b) content of *Spirogyra sp.* grown with two different initial concentrations of BPA, CR, and DCP (i.e., 5 and 50 mg/L)

EDCs	Initial concentration of chemicals (mg/L)	Biomass dry weight (mg/L)	Chlorophyll (a + b) Content (%)
Control	0	0.674 ± 0.028	79.3
BPA	5	0.686 ± 0.032	81.6
	50	0.316 ± 0.044	33.9
CR	5	0.633 ± 0.013	74.1
	50	0.323 ± 0.036	39.4
DCP	5	0.679 ± 0.021	78.8
	50	0.386 ± 0.032	47.2

3.9 Biodegradation Studies

3.9.1 The Effect of pH, and Temperature on Biodegradation Performance of BPA, CR, and DCP with MA@ALG

Biodegradation is considered as an important process to pull out the pollutant compounds from wastewaters using microorganisms. Green algae have the potential

to break down organic pollutants into small molecules (Mustafa et al., 2021). The influence of pH on the biodegradation performance of BPA, CR, and DCP with the free and MA@ALG beads was analyzed in a batch system (Fig. 10A and B). The degradation study was conducted by taking absorbance readings at the λ_{max} of the respective compounds every day for 7 days using a UV–vis spectrophotometer. The degradation performance of the algal preparations initially increased from pH 4.0 to 7.0 and then decreased from pH 6.0 to 9.0 (Fig. 10). The degradation rates of BPA, CR, and DCF with the free algal biomass were found to be 79.7%, 88.2%, and 81.7%, respectively (Fig. 10 A). As can be seen from this figure, the MA@ALG beads had a maximum degradation performance at pH 7.0 on all the tested EDCs. At pH 7.0, the degradation efficiencies of the MA@ALG were found to be 68.9%, 73.3%, and 73.4% for BPA, CR, and DCP, respectively, after a 7-day duration period at daily intervals (Fig. 10B). As can be seen from the figure, a low degradation performance was observed for all the tested EDCs compounds at alkaline pH 9.0. In this case, the oxidative enzymes of *Spirogyra sp.* were unable to function efficiently in an alkaline medium. It should be noted that the medium pH can influence the structure of the algal enzymes and the basis of their active conformational structure. Thus, for the enzyme to function properly, pH is a crucial factor. Algae can be a suitable candidate for removing and degrading phenolic compounds, playing a crucial role in the biodegradation of various toxic aromatic compounds. Generally, microorganism-based mechanisms may involve biosorption, accumulation, and degradation. The easy availability, low-cost production, favorable enzyme efficiency, and facile biomass production make algae a suitable choice for bioremediation studies involving wastewater containing organic chemicals (Otto et al., 2015; Selvan et al., 2023; Shing et al., 2018). Algal cells' surface has many different functional groups with environmentally favorable characters; thus, algae can be utilized as effective biosorbents and have a substantial role in eliminating pollutant compounds from aqueous medium through the biosorption method (Bayramoglu et al., 2018; Tahraoui et al., 2024).

The BPA, CR, and DCP-containing medium was incubated with the MA@ALG at four different temperatures, namely 15, 25, 35, and 45 °C, for a 7-day duration as described above. Data showed that MA@ALG was capable of biodegrading all the tested EDCs. The optimum growth temperature for *Spirogyra sp*. was 25 °C. Phenolic compounds degradative enzymes (laccase-like enzymes, monooxygenase, and azoreductase) are found to be more active between temperatures 25 °C and 35 °C (Aragaw, 2024). The maximum degradation of BPA, CR, and DCP was observed at 25 °C, and the MA@ALG exhibited 68.9%, 73.3%, and 73.4% degradation at 25 °C, followed by 52.2%, 66.3%, and 61.5% degradation at 45 °C, respectively. The data showed that temperatures of 15 °C and 35 °C were very close to 25 °C, and there was no significant difference (Fig. 11). Organic pollutant degradation by algae encompasses a range of enzymatic and non-enzymatic processes. Algae cells produce oxidative-specific enzymes that break down complex phenolic compounds into smaller and less toxic forms (Gerin & Remacle, 2024; Otto et al., 2015). Since algal degradative enzymes, such as laccase, peroxidase, monooxygenase, dioxygenase, hydroxylase,

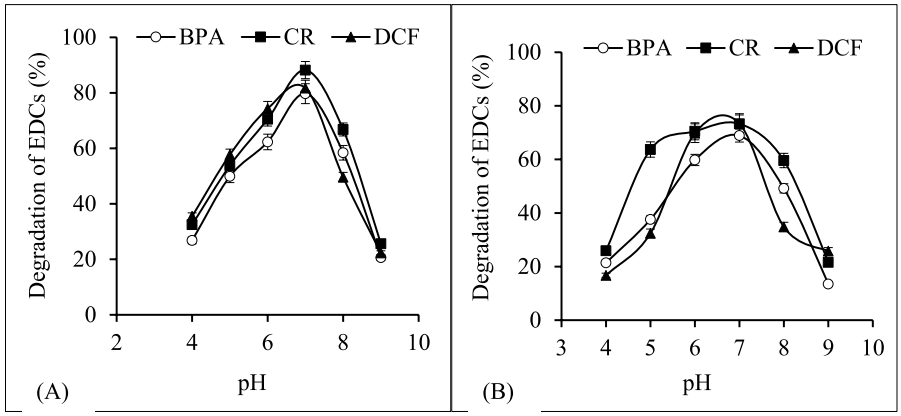


Fig. 10 Effect of pH on the degradation rate of BPA, CR, and DCP with the free algal biomass (**A**) and MA@ALG beads (**B**). (Initial concentration of ECDs compounds, 50 mg/L; pH, 4.0–9.0; temperature, 25 °C; stirring rate, 150 rpm)

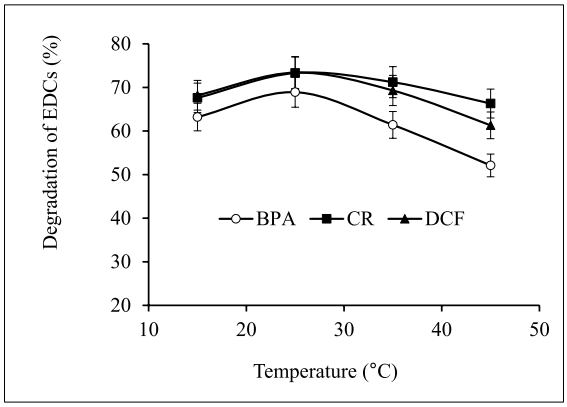


Fig. 11 Effect of temperature on the degradation rate of BPA, CR, and DCP with MA@ALG beads. (Initial concentration of each ECD compound, 50 mg/L; pH, 7.0; temperature, 15–45 °C; stirring rate, 150 rpm)

carboxylase, and decarboxylase, are important for the degradation of phenolic organic pollutants (El-Fakharany et al., 2024; Muhammad et al., 2024). It was detected that *Spirogyra sp*. was produced in the presence of the EDCs in the medium. It should be noted that laccase-like enzyme activity was not determined in the EDC-free medium and in the boiled cell-free medium, as expected for the biologically active macromolecules. Laccase enzymes are specifically oxidase syringaldazine or 2,6-dimethoxyphenol, and the presence of laccase-like activity was previously reported in *Chlamydomonas pitschmannii, Scenedesmus vacuolatus*, and *Scenedesmus ovalternus* (Gerin & Remacle, 2024; Otto & Schlosser, 2014; Otto et al., 2015). The free and entrapped *Spirogyra sp.* cells' free extract supernatants exhibited laccase activity in response to contact with EDCs. Laccase, when released into the environment, can potentially attack a broad range of phenolic compounds and break down into less toxic small molecules. This study demonstrated that Spirogyra sp. possesses laccase-like enzyme activity and may contribute to the breakdown of EDCs. A similar result was reported in an earlier work, and the substrate spectrum of green algae laccase was studied to further investigate its possible normal functions and probable significance for bioremediation (Otto et al., 2010; Pollio et al., 2005).

3.9.2 Biodegradation Study of BPA, CR, and DCF with MALDI-ToF MS

The spectra of the BPA, CR dye, and DCF achieved at the zero-point, and positive ion MALDI mass spectrum of BPA, CR, and DCF at different time intervals after treatment with MA@ALC beads are presented in Fig. 12 (partly A, B, and C, respectively). Figure 12A shows the mass spectrum of BPA in the medium, displaying two monoisotopic peaks at 251.1 m/z and 252.1. After treatment with MA@ALG beads, a marked reduction in the intensity of the BPA peaks was observed as the contact period increased with the MA@ALG preparation. In Fig. 12B, well-resolved signals of Congo red radical cation $[M^{\bullet}]^{+}$ were observed in the MALDI mass spectra, with three monoisotopic peaks at 653.1 m/z. After treatment with the material, a marked reduction in the intensity of the CR signals was noted, indicating dye degradation after 4 and 7 days of exposure. Similarly, the highly resolved monoisotopic $[M^{-2}Na^{+}3H]^{+}$ signal of, observed at 653.1 m/z, 654.1 m/z and 655.1 m/z in the MALDI mass spectra (Fig. 12B), also showed clear signs of degradation of CR after the exposure periods with MA@ALG preparation, and the observed peaks could be attributed to enzymatic degradation products, such as the diazo side chain and –NH-bonding. Figure 12C, well-resolution signals of DCF were observed in MALDI mass spectra with three monoisotopic peaks at 296.03 m/z, 297.02, and 298.02. After treatment of DCF with the MA@ALG at different time intervals, a marked reduction in the intensity of the diclofenac peaks was observed. These results provide valuable insight into the proper degradation of BPA, CR, and DCF through MA@ALG preparation, suggesting a potential approach for environmental remediation applications.

3.9.3 Reusability of the MA@ALG Beads in the Degradation of EDCs

The MA@ALG beads, after biodegradation of the pollutant compounds, can be reused or disposed of as waste materials. For the repeated use of the MA@ALG beads for degradation of BPA, CR, and/or DCF, the same preparation was used five times in a batch system. The results of the five cycles' degradation performance of BPA, CR, and/or DCF using MA@ALG beads are presented in Fig. 13. As can

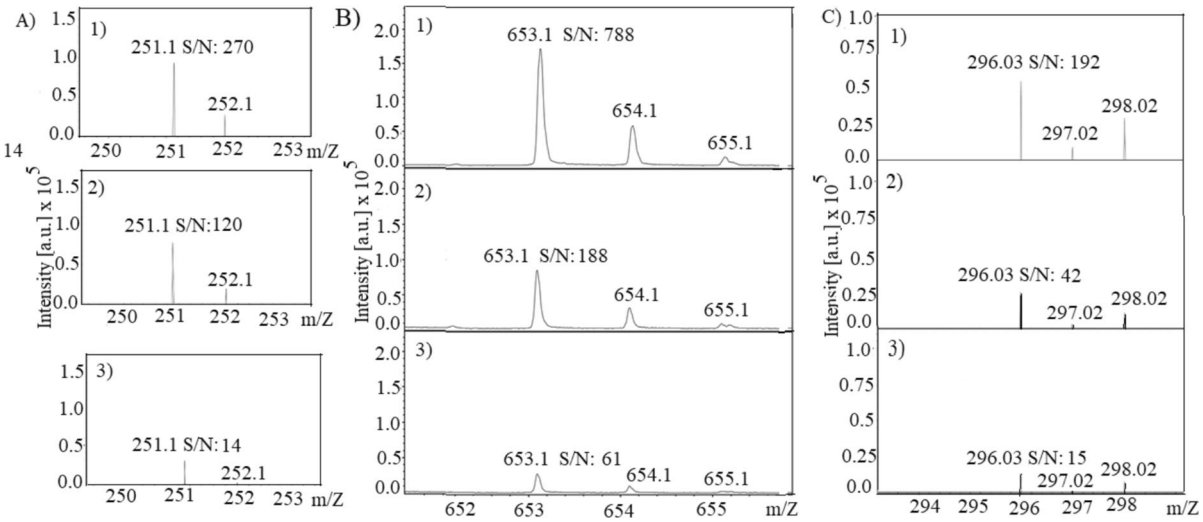


Fig. 12 (partly **A**, **B**, and **C**). High resolution MALDI mass spectra representing intensity fading of monoisotopic signal of BPA $[M+Na]^+$at the beginning of (1) at the beginning, (2) after 4 days and (3) after 7 days contact period with MA@ALG **A**. High resolution MALDI mass spectra representing intensity fading of monoisotopic signal of CR $[M\text{-}2Na+3H]^+$ (1) at the beginning of the treatment, (2) after 4 days and (3) after 7 days contact period with MA@ALG preparation **B**, High resolution MALDI mass spectra representing intensity fading of monoisotopic signal of DCF $[M+]^+$(1) at the beginning of the treatment, (2) after 4 days and (3) after 7 days contact period with MA@ALG preparation **C**. Experimental conditions: Initial concentration of each ECD compound: 25 mg/L; pH: 7.0; temperature: 25 °C; stirring rate: 150 rpm

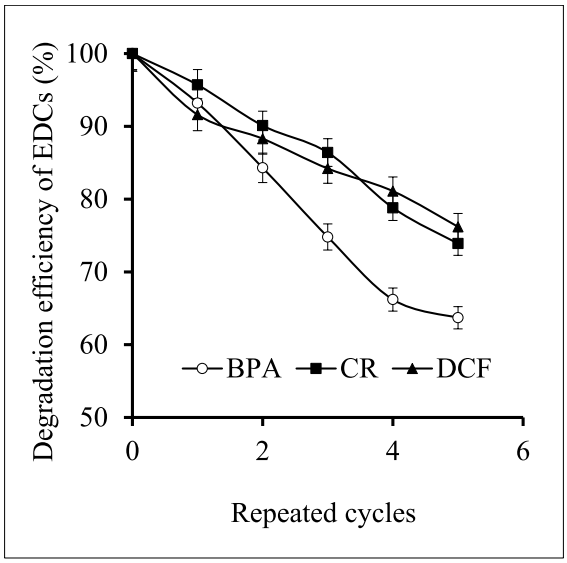


Fig. 13 Repeated use of the MA@ALG beads for biodegradation of BPA, CR, and DCP in a batch system. (Initial concentration of ECDs compounds, 50 mg/L; pH, 7.0; temperature, 25 °C; stirring rate, 150 rpm)

be seen from this figure, the degradation efficiency of BPA, CR, and DCF using the MA@ALG beads was reduced by about 36.3%, 26.1%, and 23.8%, respectively, after five reuse in a batch system compared to their initial degradation performance. After each repeated run, the MA@ALG beads were separated from the batch system and washed with sterile saline solution (0.85%). The MA@ALG beads were incubated in BBG medium for 24 h, and then the same regenerated MA@ALG beads were operated in the next degradation cycle for seven days.

3.10 Toxicity Studies

3.10.1 Daphnia Magna Death Rate

The toxic contaminants in water can be evaluated using different living test organisms, which serve as a natural toxicity meter. Among them, the assessment of Daphnia magna death rates is frequently used for determining the toxicity of chemicals (Bayramoglu et al., 2019). The toxic effects of the degradation products of BPA, CR, and/or DCF, obtained using the MA@ALG preparations, were studied in the freshwater crustacean D. magna over 48 h contact time

periods, with respective pure compounds used as controls. D. magna mortality test is very sensitive to many toxic compounds, and the result can be rapidly obtained. The influences of BPA, CR, and DCF concentrations on *D. magna* mortality rates were studied over 48 h exposure periods to each test compound, and the toxicities of BPA, CR, and DCF for D. magna were determined to be 11.9, 15.3, and 32.5 mg/L, respectively. The EC_{50} concentration values for BPA, CR, and DCF after 48 h were calculated to be 6.84, 7.07, and 18.9 mg/L, respectively. After treatment of the medium containing BPA, CR, and DCF with the MA@ALG preparation, in the remaining medium, no toxic effects were observed on *D. magna* due to the biodegradation of all the tested chemicals by the MA@ALG.

3.10.2 Microalgae Growth Inhibition Test

Chlamydomonas reinhardtii is a unicellular green algae, and it is very sensitive to phenolic pollutants (Bayramoglu et al., 2019). The toxicities of BPA, CR, DCF, and their degradation products were evaluated on the viability of *C. reinhardtii* by varying the concentrations of each tested pollutant between 5 and 50 mg/L. The results are presented in Table 4. The decrease in the growth efficiency of *C. reinhardtii* was more pronounced as the concentration of the pollutants increased. After a 10-day incubation with BPA, CR, and DCF, the amount of biomass of *C. reinhardtii* was significantly reduced for all the tested phenolic pollutants, and the amount of biomass of *C. reinhardtii* incubated with 50 mg/L of individual solutions of BPA, CR, and DCF was found to be 0.187, 0.293, and 0.562 g/L, respectively. The amount of *C. reinhardtii* biomass in the control culture after ten-day cultivation was found to be 1.128 g/L dry weight. The amounts of algal biomass were reduced by approximately 6.03, 3.85, and 2.01-fold after 10-day incubation with BPA, CR, and DCF, respectively, compared to the control alga culture. The order of the effect of pollutants on the reduction of algal biomass was BPA > CR > DCF. As shown in this table, BPA, CR, and DCF degradation products exhibited no toxic properties, and the amounts of algal biomass obtained were very similar to those of the control group. These results may provide helpful information to determine the risk of toxicity of phenolic pollutants on the growth performance of the algal species, and also offer valuable insights for future studies.

3.10.3 Phytotoxicity Studies with Tested Phenolic Pollutants

The phytotoxicity of the EDCs (i.e., BPA, CR, and DCF) before and after contact with MA@ALG in a batch system was assessed and determined using the germination index (GI) with Turkish winter wheat (*Triticum aestivum L.*) seeds. The control freshwater medium had no toxic effects on the growing Turkish winter wheat seeds. The germination rate of Turkish winter wheat seeds decreased after contact with each tested pollutant (i.e., BPA, CR, and DCF at 50 mg/L concentrations), and the germination rate in fresh water was assumed as 100% and decreased after contact of the seeds with each pollutant approximately 69, 47, and 38%, respectively. For root lengths of the seeds less than 5 mm, it was observed that they did not germinate; however, the germination index improved after ten days. When the Turkish winter wheat seed was incubated after treatment of BPA, CR, and DCF solutions with the MA@ALG, the plant's growth was not affected by the degradation products of the tested pollutants, as compared to the growth of the control seeds. These examinations correlated the detoxification of BPA, CR, and DCF pollutants with the MA@ALG. It was observed that after treatment with algal biomass, no toxic elements remained in the solutions, and the germination of the wheat seeds was the same in each treated pollutant as in the freshwater controls. Similar observations for azo dyes have been reported, such as the damaging properties of textile discharge having azo dyes on seed germination, which were studied using groundnut seed (Zhoua & Xiang, 2013; de Almeida et al., 2021), and after treatment of the effluent with fungal consortium KCMN-13 the germination rate was the same with treated textile effluent as control top water.

4 Conclusions

In this study, the biosorption and biodegradation abilities of MA@ALG were investigated using free algal biomass as a control system. In this work, the algae "Spirogyra sp." was selected and used because of it could be easily isolated from a

freshwater supply, and also degraded many organic chemicals from aqueous solution under favorable conditions. The MA@ALG was well characterized by FT-IR, SEM, and analytical methods. The MA@ALG exhibited high biosorption capacity for BPA, CR, and DCP, and also effectively degraded these compounds. The entrapped *Spirogyra* cells in the alginate gel remained alive during the biosorption and biodegradation studies. The biosorption capacities of the algal biomass preparations were influenced by various experimental conditions, including the biosorbent dosage, medium pH, and temperature. The maximum biosorption capacity of the MA@ALG was found to be 73.6, 104.4, and 49.5 mg/g for BPA, CR and DCF, respectively. Whereas the biosorption capacity of the free algal biomass at pH 7.0 for BPA, and CR, DCF was 89.4, 163.1, and 68.2 mg/g, respectively. The biosorption of BPA, CR, and DCP on both algal preparations was well described by the Langmuir isotherm model, and the biosorption kinetics followed the pseudo-first-order model. As reported earlier, phenolic compounds such as EDCs can be enzymatically broken down by laccases present in most green algae. The algae laccase enzymes are generally active at a neutral pH, similar to plant laccase, for the oxidation of phenolic compounds. In this work, laccase-like enzyme activity was detected in *Spirogyra* cells and should be involved in the degradation of the tested endocrine-disturbing compounds. The MA@ALG beads were operated in consecutive five cycles in a batch system for the degradation of BPA, CR, and DCP, and the degradation efficiency decreased to 63.7%, 73.9%, and 76.2% for BPA, CR, and DCP, respectively. Furthermore, the degradation efficiency of the MA@ALG beads was also reduced when the concentrations of BPA, CR, and DCP were increased from 5 mg/L to 50 mg/L in the medium. The potential toxicity of pure BPA, CR, and DCP and their biodegradation products on D. magna and Turkish winter wheat Triticum aestivum L. was studied, and it was found that pure BPA, CR, and DCP had toxic effects on the test organism, while their degradation products did not show any toxic effects on the test organisms. Thus, the biodegradation products of BPA, CR, and DCP allowed for an understanding of the toxicity of EDCs before and after degradation by MA@ALG. As observed from algae growth tests, at high concentrations of EDCs, the growth of the algae was suppressed compared to the control groups due to the toxicity of these chemicals. From these observations, algal-based systems can be used to degrade harmful chemicals into a non-toxic form, providing a cost-effective solution, and the treated wastewater can be reused or released into the environment.

Author Contributions Gulay Bayramoglu: Methodology, Investigation, Validation, Formal analysis, Resources, Writing – original draft, Writing – review & editing. Ilkay Erkaya Acikgoz: Methodology, Investigation, Resources, Writing–original draft. Omur Celikbicak: Methodology. Investigation, M. Yakup Arica: Project administration, Conceptualization, Writing—review & editing.

Funding Open access funding provided by the Scientific and Technological Research Council of Türkiye (TÜBİTAK). This work was supported by Kırşehir Ahi Evran University and Gazi University. Kırşehir Ahi Evran University, BAP, Project Number: MMF.A2.24.002.

Data Availability All data generated or analyzed during this study are included in the article, and also provided upon request.

Declarations

Ethics Approval Not applicable.

Consent for Publication The participant has consented to the submission of the study to the journal.

Competing Interests We declare that this is an original research work of the authors and all the authors have contributed to the completion of this work, which is embedded in this paper. We also confirm that this work has not been published elsewhere nor it is currently under consideration for publication elsewhere. We have no conflict of interest.

Open Access This article is licensed under a Creative Commons Attribution 4.0 International License, which permits use, sharing, adaptation, distribution and reproduction in any medium or format, as long as you give appropriate credit to the original author(s) and the source, provide a link to the Creative Commons licence, and indicate if changes were made. The images or other third party material in this article are included in the article's Creative Commons licence, unless indicated otherwise in a credit line to the material. If material is not included in the article's Creative Commons licence and your intended use is not permitted by statutory regulation or exceeds the permitted use, you will need to obtain permission directly from the copyright holder. To view a copy of this licence, visit http://creativecommons.org/licenses/by/4.0/.

References

Alexander, H., Dill, D. C., Smith, W., Guine, P. D., & Dorn, P. (1988). Bisphenol A: Acute aquatic toxicity. *Environmental Toxicology and Chemistry, 7*, 19–26. https://doi.org/10.1002/etc.5620070104

Al-Tohamy, R., Ali, S. S., Li, F., Okasha, K. M., Mahmoud, Y.-G., Elsamahy, T., Jiao, H., Fu, Y., & Sun, J. (2022). A critical review on the treatment of dye-containing wastewater: Ecotoxicological and health concerns of textile dyes and possible remediation approaches for environmental safety. *Ecotoxicology and Environmental Safety, 231*, Article 113160. https://doi.org/10.1016/j.ecoenv.2021.113160

Aragaw, T. A. (2024). A review of dye biodegradation in textile wastewater, challenges due to wastewater characteristics, and the potential of alkaliphiles. *Journal of Hazardous Materials Advances, 16*, Article 100493. https://doi.org/10.1016/j.hazadv.2024.100493

Arica, M. Y., & Bayramoglu, G. (2016). Polyaniline coated magnetic carboxymethylcellulose beads for selective removal of uranium ions from aqueous solution. *Journal of Radioanalytical and Nuclear Chemistry, 310*, 711–724. https://doi.org/10.1007/s10967-016-4828-z

Arica, M. Y., Salih, B., Celikbicak, O., & Bayramoglu, G. (2017). Immobilization of laccase on the fibrous polymer grafted film and studies of textile dyes degradation by MALDI-ToF-MS. *Chemical Engineering Research & Design, 128*, 107–119. https://doi.org/10.1016/j.cherd.2017.09.023

Arica, T. A., Ayas, E., & Arica, M. Y. (2017b). Magnetic MCM-41 silica particles grafted with poly(glycidylmethacrylate) brush: Modification and application for removal of direct dyes. *Microporous and Mesoporous Materials, 243*, 164–175. https://doi.org/10.1016/j.micromeso.2017.02.011

Arica, T. A., Balci, F. M., Balci, S., & Arica, M. Y. (2022). Highly porous poly(*o*-phenylenediamine) loaded magnetic carboxymethyl cellulose hybrid beads for removal of two model textile dyes. *Fibers and Polymers, 23*, 2838–2854. https://doi.org/10.1007/s12221-022-0221-4

Bayramoglu, G., & Arica, M. Y. (2011). Preparation of a composite biosorbent using *Scenedesmus quadricauda* biomass and alginate/polyvinyl alcohol for removal of Cu(II) and Cd(II) ions: Isotherms, kinetics, and thermodynamic studies. *Water, Air, and Soil Pollution, 221*, 391–403. https://doi.org/10.1007/s11270-011-0798-5

Bayramoglu, G., & Arica, M. Y. (2023). Biodegradation studies of phenol, diclofenac, and pentachlorophenol in a packed bed reactor loaded with immobilized white rot fungus *Lentinus sajor-caju* biomass. *Water, Air, and Soil Pollution, 234*, Article 620. https://doi.org/10.1007/s11270-023-06634-9

Bayramoglu, G., & Arica, M. Y. (2024). Agmatine ligand functionalized magnetic alginate beads for removal of U(VI) ions from solution. *Journal of Radioanalytical and Nuclear Chemistry, 333*, 4197–4210. https://doi.org/10.1007/s10967-024-09548-w

Bayramoglu, G., Akbulut, A., Acıkgoz-Erkaya, I., & Arica, M. Y. (2018). Uranium sorption by native and nitrilotriacetate-modified *Bangia atropurpurea* biomass: Kinetics and thermodynamics. *Journal of Applied Phycology, 30*, 649–661. https://doi.org/10.1007/s10811-017-1238-8

Bayramoglu, G., Salih, B., Akbulut, A., & Arica, M. Y. (2019). Biodegradation of Cibacron Blue 3GA by insolubilized laccase and identification of enzymatic byproduct using MALDI-ToF-MS: Toxicity assessment studies by *Daphnia magna* and *Chlorella vulgaris*. *Ecotoxicology and Environmental Safety, 170*, 453–460. https://doi.org/10.1016/j.ecoenv.2018.12.014

Bayramoglu, G., Angi, S. B., Acikgoz-Erkaya, I., & Arica, M. Y. (2022). Preparation of effective green sorbents using *O. princeps* alga biomass with different composition of amine groups: Comparison to adsorption performances for removal of a model acid dye. *Journal of Molecular Liquids, 347*, Article 118375. https://doi.org/10.1016/j.molliq.2021.118375

Bayramoglu, G., Kilic, M., & Arica, M. Y. (2023). *Trametes trogii* biomass in carboxymethyl cellulose-lignin composite beads for adsorption and biodegradation of bisphenol A. *Biodegradation, 34*, 263–281. https://doi.org/10.1007/s10532-023-10024-7

Cai, Y., Qiu, C., Yang, K., Tian, B., & Bi, Y. (2024). Adsorption–degradation of methylene blue by natural manganese ore: Kinetics, characterization, and mechanism. *International Journal of Environmental Science and Technology, 21*, 1817–1830. https://doi.org/10.1007/s13762-023-05024-2

Celikbicak, O., Bayramoglu, G., Yilmaz, M., Bicak, N., Salih, B., & Arica, M. Y. (2014). Immobilization of laccase on hairy polymer grafted zeolite particles: Degradation of a model dye and product analysis with MALDI-ToF-MS. *Microporous and Mesoporous Materials, 199*, 57–65. https://doi.org/10.1016/j.micromeso.2014.08.003

Chaturvedi, A., & Jaiswal, R. P. (2023a). Investigation of external mass transfer during biodegradation of Congo red dye in a recirculating packed bed bioreactor. *Water, Air, and Soil Pollution, 234*, Article 360. https://doi.org/10.1007/s11270-023-06382-w

Chaturvedi, A., & Jaiswal, R. P. (2023). Investigation of external mass during biodegradation of congo red dye in a recirculating packed bed bioreactor. *Water, Air, and Soil Pollution, 234*, Article 360. https://doi.org/10.1007/s11270-023-06382-w

Daniel, S. F. J., Cardoso, F. R., Angilelli, K. B., Gomes, C. A., Abreu, L. M., & Carvalho, J. O. (2025). *Trametes cingulata*: A white rot fungus in decolorization of azo dye Reactive red 239. *Journal Chemical Technology Biotechnology, 100*, 577–590. https://doi.org/10.1002/jctb.7797

de Almeida, A. P., Macrae, A., Ribeiro, B. D., & do Nascimento, R. P. (2021). Decolorization and detoxification of different azo dyes by *Phanerochaete chrysosporium* ME-446 under submerged fermentation. *Brazilian Journal of Microbiology, 52*, 727–738. https://doi.org/10.1007/s42770-021-00458-7

de Wilt, A., Butkovskyi, A., Tuantet, K., Leal, L. H., Fernandes, T. V., Langenhoff, A., & Zeeman, G. (2016). Micropollutant removal in an algal treatment system fed with source separated wastewater streams. *Journal of Hazardous Materials, 304*, 84–92. https://doi.org/10.1016/j.jhazmat.2015.10.033

El-Fakharany, E. M., Saleh, A. K., El-Maradny, Y. A., El-Sayed, M. H., Alali, I., Alsirhani, A. M. A., Alalawy, I., Alhawiti, A. S., Alatawi, I. S., Mazi, W., & El-Gendi, H. (2024). Comprehensive insight into recent algal enzymes production and purification advances: Toward effective commercial applications: A review. *International Journal of Biological Macromolecules, 283*, Article 137783. https://doi.org/10.1016/j.ijbiomac.2024.137783

Gerin, S., & Remacle, C. (2024). Efficient secretion of a true laccase by the acidophilic green microalga *Chlamydomonas pitschmannii* switched to alkaline pH. *Journal of Applied Phycology, 36*, 2545–2557. https://doi.org/10.1007/s10811-024-03299-7

Ghibate, R., Chrachmy, M., Alaqarbeh, M., Ansari, A., Baaziz, M. B., Bouachrine, M., Taouil, R., & Senhaji, O. (2025). Comprehensive analysis of hazardous dye adsorption onto a green adsorbent: Experimental profiling, theoretical modeling, and deciphering potential molecular interactions. *Desalination and Water Treatment, 321*, Article 100998. https://doi.org/10.1016/j.dwt.2025.100998

Gode, J. N., Malaret, F. J., Hallett, J. P., Trevisan, V., & Skoronski, E. (2024). Phosphonium-based ionic liquid immobilized in sodium alginate as a novel adsorbent: Kinetics, thermodynamics, and toxicity study on 2,4-dichlorophenol removal. *Chemical Engineering Research and Design, 205*, 161–173. https://doi.org/10.1016/j.cherd.2024.03.030

González-López, F., Alonso-Molina, J. L., Mendoza-Roca, J. A., Cuartas-Uribe, B., Rendón-Castrillón, L., Ocampo-López, C., & Ramírez-Carmona, M. (2024). Native microorganisms for sustainable dye biodegradation in wastewaters from jeans finishing. *Environmental Science and Pollution Research, 31*, 64675–64687. https://doi.org/10.1007/s11356-024-35563-1

Khazaali, F., Kargari, A., & Rokhsara, M. (2014). Application of low-pressure reverse osmosis for effective recovery of bisphenol A from aqueous wastes. *Desalination and Water Treatment, 52*, 7543–7551. https://doi.org/10.1080/19443994.2013.831795

Kumari, S., Singh, R., Jahangeer, J., & Garg, M. C. (2024). Innovative strategies for dye removal from textile wastewater: A comprehensive review of treatment approaches and challenges. *Water, Air, and Soil Pollution, 235*, Article 720. https://doi.org/10.1007/s11270-024-07532-4

Li, K., Lai, Y., Lin, S., Zhou, L., He, M., Lin, H., & Yuan, Y. (2024). Contact-electro-catalysis for the degradation of pentachlorophenol using inert fluorinated ethylene propylene powders. *ACS ES & T Engineering, 4*, 2485–2494. https://doi.org/10.1021/acsestengg.4c00284

Liang, J., Zhang, C. M., & Zhu, C. C. (2024). Toxic effects and mechanisms of cationic blue SD-GSL on *Chlorella vulgaris* before and after the biological decolorization process. *Chemosphere, 349*, Article 140947. https://doi.org/10.1016/j.chemosphere.2023.140947

Lilhare, S., Mathew, S. B., Singh, A. K., & Carabineiro, S. A. C. (2021). Calcium alginate beads with entrapped iron oxide magnetic nanoparticles functionalized with methionine—A versatile adsorbent for arsenic removal. *Nanomaterials, 11*, Article 1345. https://doi.org/10.3390/nano11051345

Modi, A., Baranda, P., Thakor, R., Thacker, D., Trivedi, J., & Bariya, H. (2025). Fungal consortium mediated efficient biodegradation of hazardous reactive dyes from textile effluent: An environmentally acceptable strategy. *Journal of Hazardous Materials Advances, 18*, Article 100705. https://doi.org/10.1016/j.hazadv.2025.100705

Moja, M. M., Mapossa, A. B., Chirwa, E. M. N., & Tichapondwa, S. (2024). Photocatalytic degradation of 2,4-dichlorophenol using nanomaterials silver halide catalysts. *Environmental Science and Pollution Research, 31*, 11857–11872. https://doi.org/10.1007/s11356-024-31921-1

Muhammad, M. A., Balogun, E. O., Sallau, A. B., Chia, M. A., & Shuaibu, M. N. (2024). Identification of novel laccase from cyanobacterium *Microcystis flos-aquae* and enhanced azo dye bioremediation potential. *Bioresource Technology, 399*, Article 130587. https://doi.org/10.1016/j.biortech.2024.130587

Mustafa, S., Bhatti, H. N., Maqbool, M., & Iqbal, M. (2021). Microalgae biosorption, bioaccumulation and biodegradation efficiency for the remediation of wastewater and carbon dioxide mitigation: Prospects, challenges and opportunities. *Journal of Water Process Engineering, 41*, Article 102009. https://doi.org/10.1016/j.jwpe.2021.102009

O.E.C.D, 2004. Acute Immobilization Test, Daphnia sp., OECD Guideline for the testing of chemicals, Guideline 202

O.E.C.D, 2011. Freshwater Alga and Cyanobacteria, Growth Inhibition Test. OECD Guideline for the testing of chemicals, Guideline

Otto, B., & Schlosser, D. (2014). First laccase in green algae: Purifcation and characterization of an extracellular phenol oxidase from *Tetracystis aeria*. *Planta, 240*, 1225–1236. https://doi.org/10.1007/s00425-014-2144-9

Otto, B., Schlosser, D., & Reisser, W. (2010). First description of a laccase like enzyme in soil algae. *Archieve Microbiolgy, 192*, 759–768. https://doi.org/10.1007/s00425-014-2144-9

Otto, B., Beuchel, C., Liers, C., Reisser, W., Harms, H., & Schlosser, D. (2015). Laccase-like enzyme activities from *Chlorophycean* green algae with potential for bioconversion of phenolic pollutants. *FEMS Microbiology Letters, 362*, Article fnv072. https://doi.org/10.1093/femsle/fnv072

Pollio, A., Cennamo, P., Ciniglia, C., De Stefano, M., Pinto, G., & Huss, V. A. (2005). Chlamydomonas pitschmannii Ettl, a Little Known Species from Thermoacidic Environments. *Protist, 156*, 287. https://doi.org/10.1016/j.protis.2005.04.004

Porra, R. J., Thompson, W. A., & Kriedemann, P. E. (1989). Determination of accurate extinction co-efficient and simultaneous-equations for assaying chlorophyll a+b extracted with 4 different solvents – Verification of the concentration of chlorophyll standards by atomic-absorption spectroscopy. *Biochimica et Biophysica Acta, 975*, 384–394. https://doi.org/10.1016/S0005-2728(89)80347-0

Rajaselvam, J., Kadaikunnan, S., Alharbi, N. S., Khaled, J. M., & Vijayaraghavan, P. (2024). Biodegradation of endocrine disrupting compounds from the wastewater by the immobilized indigenous bacteria. *Environmental Quality*

Management, 34, Article e22252. https://doi.org/10.1002/tqem.22252

Saravanan, A., Yaashikaa, P. R., Ramesh, B., Alan, S., & Deivayanai, V. C. (2024). Microorganism-mediated bioremediation of dyes from contaminated soil: Mechanisms, recent advances, and future perspectives. *Food and Chemical Toxicology, 185*, Article 114491. https://doi.org/10.1016/j.fct.2024.114491

Selvan, B. K., Pandiyan, R., Vaishnavi, M., Das, S., & Thirunavoukkarasu, M. (2023). Ameliorative biodegradation of hazardous textile industrial wastewater dyes by potential microalgal sp. *Biomass Conversion and Biorefinery, 13*, 13481–13492. https://doi.org/10.1007/s13399-022-02725-5

Semwal, N., Mahar, D., Chatti, M., Kumar, R., & Arya, M. C. (2024). Ni-Zn/CeO_2 nanocomposites for enhanced adsorptive removal of 4-chlorophenol. *Environmental Science and Pollution Research, 31*, 51934–51953. https://doi.org/10.1007/s11356-024-34669-w

Shing, W. L., Hwang, T. Y., Yi, K. W., Han, L. J., & Hock, O. G. (2018). Using the responses of green algae *Spirogyra* as bioindicator for metals and pesticides pollution. *Journal of Environmental Science and Management, 21*, 1–6. https://doi.org/10.47125/jesam/2018_2/01

Shtein, I., Bar-On, B., & Popper, Z. A. (2018). Plant and algal structure: From cell walls to biomechanical function. *Physiologia Plantarum, 164*, 56–66. https://doi.org/10.1111/ppl.12727

Tahraoui, H., Belhadj, A. E., Amrane, A., Toumi, S., Jaouadi, B., & Zhang, J. (2024). Maximizing diclofenac bioremoval efficiency using *Chlorella vulgaris* strain H1 and *Chlorella sorokiniana* strain H2: Unveiling the impact of acetic acid on microalgae. *Institute of Chemical Engineers, 165*, Article 105783. https://doi.org/10.1016/j.jtice.2024.105783

Touliabah, H. E. S., El-Sheekh, M. M., Ismail, M. M., & El-Kassas, H. (2022). A review of microalgae- and cyanobacteria-based biodegradation of organic pollutants. *Molecules, 27*, Article 1141. https://doi.org/10.3390/molecules27031141

Wijaya, A., Ahmad, N., Hanum, L., Melwita, E., & Lesbani, A. (2025). *Spirogyra sp.* macro-algae-supported NiCr-LDH adsorbent for enhanced Remazol red dye removal. *Results in Surfaces and Interfaces, 18*, Article 100427. https://doi.org/10.1016/j.rsurfi.2025.100427

Wlizło, K., Siwulski, M., Kowalska-Krochmal, B., & Wiater, A. (2024). Exploring the potential of fungal biomass for bisphenol A removal in aquatic environments. *International Journal of Molecular Sciences, 25*, Article 11388. https://doi.org/10.3390/ijms252111388

Xiong, J. Q., Kurade, M. B., & Jeon, B. H. (2018). Can microalgae remove pharmaceutical contaminants from water? *Trends in Biotechnology, 36*, 30–44. https://doi.org/10.1016/j.tibtech.2017.09.003

Zhoua, X., & Xiang, X. (2013). Effect of different plants on azo-dye wastewater biodecolorization. *Procedia Environmental Sciences, 18*, 540–546. https://doi.org/10.1016/j.proenv.2013.04.073

Publisher's Note Springer Nature remains neutral with regard to jurisdictional claims in published maps and institutional affiliations.